

Master Thesis

Die approbierte Originalversion dieser Diplom-/Masterarbeit ist an der Hauptbibliothek der TU Wien in Central & Eastern Europe (http://www.ub.tuwien.ac.at).

The approved original version of this diploma or master thesis is available at the main library of the Vienna University of Technology (http://www.ub.tuwien.ac.at/englweb/).



Development of a measurement process for in situ testing of amorphous silicon thin-film multi junction photovoltaic degradation and measured data based potential comparison of second generation PVs

A Master's Thesis submitted for the degree of
"Master of Science"

Supervised by
Dipl.Ing. Hubert Fechner, MAS, MSc.

Szentannai György

0927429

31 October 2011, Budapest

Master Thesis

MSc Program
Renewable Energy in Central & Eastern Europe

Affidavit

I, **Szentannai György**, hereby declare

that I am the sole author of the present Master Thesis, "Development of a measurement process for in situ testing of amorphous silicon thin-film multi junction photovoltaic degradation and measured data based potential comparison of second generation PVs"

1. 54 pages, bound, and that I have not used any source or tool other than those referenced or any other illicit aid or tool, and
2. that I have not prior to this date submitted this Master Thesis as an examination paper in any form in Austria or abroad.

Vienna, _____

Date

Signature

Abstract

Thin film photovoltaic cells are a widely used, second generation electricity generation system. Aside from many economical and ecological advantages, the main limitation of amorphous thin film cells is that light induced degradation occurs in the first months of sun exposure. As light induced degradation has still not been fully understood, research focus on alternative solutions. Two such products that were recently introduced and disseminated widely on the market are used as a subject to develop a comparison method in situ circumstances. The real performance and degradation of newly implemented micromorph cells were tested at private houses in Niederösterreich and in Vienna. Their productivity was economically compared with that of a hetero-junction cell.

Even if, as is to be expected in an in situ trial, two locations out of four were filed, the calculated results are in parallel with the literature and are slightly behind the producers' data.

Table of Content

1	Introduction	7
1.1	Motivation	7
1.1.1	Renewable market	8
1.1.2	PV development, potential	9
1.2	Core objective	10
1.2.1	Live productivity of second generation multi-junction PV's	10
1.2.2	The target of this thesis	10
1.2.3	Method of measurement development	11
1.3	Citation of main literature	11
1.3.1	PV basement of photovoltaic electricity production	11
1.3.2	Type of silicon PVs	12
1.3.3	Efficiency, degradation	14
2	Description of method of approach applied	17
2.1	Elements of method	17
2.2	Data of producers	18
2.3	Expectations based on relevant literature	20
2.3.1	Productivity and efficiency	20
2.3.2	Expectations of degradation curve	24
2.4	Targets of measurements: calculate degradation, present real production	28
2.5	Calculation method of degradation	29
2.6	Method of complementary calculation (NPV)	32
3	Documentation of data and data collection	33
3.1	Description of the in situ measurements	33
3.2	Data and results of the measurements	35
3.3	Description of Sanyo data sources	36
4	Description of results	37
4.1	Efficiency and production comparison of producers data and measured data	38

Master Thesis

MSc Program
Renewable Energy in Central & Eastern Europe

4.2	Discussion of the results	38
5	Conclusion	41
6	References	43
7	Annexes	46
7.1	Meteorology data of the locations	46
7.2	Definition of some photovoltaic terminology	47

List of tables and figures

Table 1	Top efficiency of different type solar cells	24
Table 2	“Weak light performance” of Bosch μ -Si plus 115 by the producer.	31
Table 3	The list and accuracy of the used instruments	35
Table 4	The main initial data of in situ measurements	36
Table 5	Calculated relative initial granted production data under Standard Test Condition of the panels	36
Table 6	Measured data after 3 months summer sun degradation panels and its calculated relative productivity and efficiency.	37
Figure 1	Average annual growth rates of renewable energy capacity (2005-2010)	8
Figure 2	Conversion efficiency of different band gap semiconductors. The band gap of amorphous silicon fits the solar spectrum better than that of crystalline silicon	15
Figure 3	Hydrogen collision model assumes that the degradation caused by a loose hydrogen atoms which can open weak silicon-silicon bond	17
Figure 4	Sanyo HIT cell heterojunction structure. Mono crystalline silicon is combined with n and p type amorphous silicons	18
Figure 5	Data sheets of Bosch μ -Si plus 115 and Sanyo HIT Power 115	20
Figure 6	Best research PV cell efficiencies of different type of cells	23
Figure 7	Seasonal efficiency alternation of amorphous silicon PVs: degradation and regeneration of single junction (Si-1) and triple junction (Si-2 and Si-3) amorphous silicon solar cells in South Africa. Section A: first month of sun explosion, Section B and D: colder winter period, Section C and E warmer summer period.	26
Figure 8	Average temperature, irradiation and sunshine hours differences of the four test locations	28
Figure 9	ΔU_{mpp} and ΔI_{mpp} correlation to φ	31
Figure 10	The installation of Bosch μ -Si plus 115 in Gutenstein and the irradiation measurement.	34

Master Thesis

MSc Program

Renewable Energy in Central & Eastern Europe

Figure 11	Relative productivity differences Gutenstein after 1 ½ month of sun exposition	40
Figure 12	Sunshine differences of the locations	46
Figure 13	Average temperatures of the locations	47
Figure 14	Fill factor	48
Figure 15	I-U (J-V) characteristics of $\mu\text{-Si:H}$ single-junction solar cells versus the intrinsic layer thickness	50
Figure 16	The amorphous-microcrystalline formation, transaction and thickness growth related to R ($R = [\text{H}]/[\text{SiH}_4]$) ratio and nucleation density (N_d).	54

1 Introduction

1.1 Motivation

The 2009-2010 global economic recessions led to public finance crises and cutbacks by several governments in renewable and especially solar energy investment. At the same time the economic recession worldwide highlighted the importance of energy supply security and becoming energetically independent. Also, the Fukushima tragedy in 2011 represented a serious warning, at least in the European continent, regarding nuclear power usage.

The first generation crystalline silicon based photovoltaic modules have higher efficiency than amorphous silicon based thin films. There are many reasons for this efficiency difference, such as crystalline being free of grain boundaries, which decreases conductivity and light induced efficiency degradation. Light induced efficiency degradation was first reported more than 40 years ago. Since that time the Staebler-Wronsky effect (SWE), which is reversible by heat treatment, has still not been totally understood. On the other hand amorphous silicon based PV has many advantages compared to crystalline:

- cheaper production cost, because less raw material is used during its manufacture. The total a-Si:H thickness is typically 50 nm compared to wafer thickness of several hundreds (300-500 μm) microns.
- cheaper production cost due to its much lower manufacturing temperature. While crystalline silicon production temperature is on 800-1000 $^{\circ}\text{C}$ than the amorphous silicon production temperature is around 200 $^{\circ}\text{C}$.
- much shorter environmental pay-back time in the sense of investigated and gathered CO_2 emission, reduction of production during the life time and savings.
- amorphous PVs maintain their efficiency at higher temperatures better than traditional crystalline
- amorphous silicon solar panels have higher quantum efficiency in lower wave length (0,5-0,6 μm), while crystalline silicon optimal spectrum intensity is at higher (0,8-1,0 μm) wave length. This means thin-film amorphous solar panels function is not that dominant in direct sunshine, it has significant advantages on cloudy days.

There are intensive research and development efforts to understand the Staebler-Wronsky effect more accurately to reap amorphous silicon PV's advantages. The advantages discussed above force producers to use amorphous silicon panels of different types, in different combinations, like in multi-junction PVs. It is important for the implementation

Master Thesis

MSc Program
Renewable Energy in Central & Eastern Europe

companies and also for consumers to know the real degradation time and percentage in applied practice.

The expected result should be mainly to see the real electricity production of the newest developed multi-junction silicon PVs production compared to results in the literature and the producers' data.

1.1.1 Renewable market

The renewable market is part of one of the largest world markets: the energy market. It is not yet a totally open market, due to different direct state motivations. Even so, investment in renewable energy in the past decade shows a continuous, significant increase. This growth is shown by the main sectors on the Figure 1.

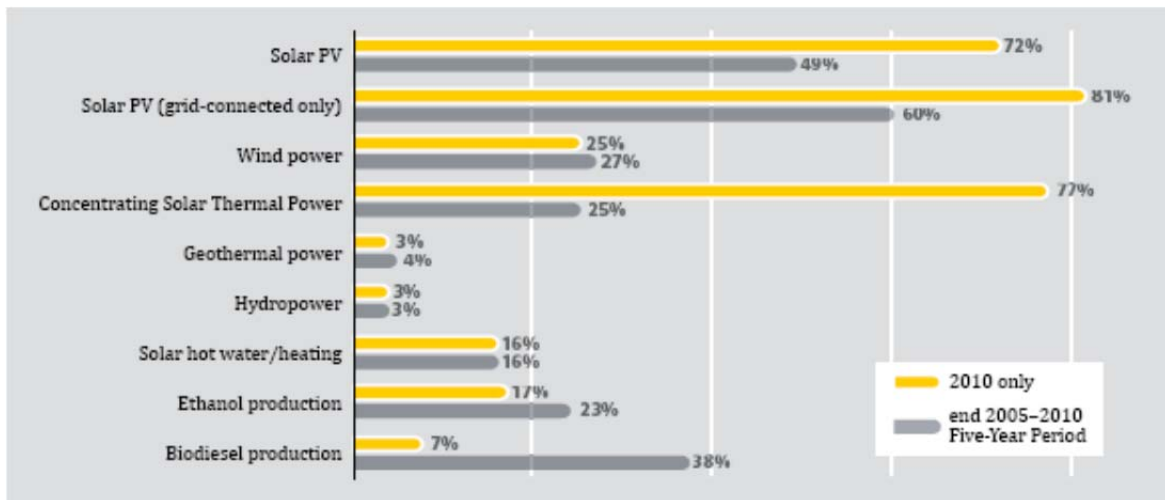


Figure 1: Average annual growth rates of renewable energy capacity (2005-2010)
Renewables 2011 Global Status Report

Renewable sources have grown to supply an estimated 20% of global final energy consumption in 2010. By year's end, renewable comprised one-quarter of global power capacity from all sources and delivered close to one-fifth of the world's power supply. Most technologies held their own, despite the challenges faced, while solar PV surged with more than twice the capacity installed as the year before.

Renewable energy accounted for approximately half of the estimated 194 gigawatts (GW) of new electric capacity added globally during the year 2010.

In several countries renewable represents a high share of energy consumption and is increasing rapidly: China added 29 GW of grid connected renewable capacity for a total of 263 GW. Renewable accounted for about 26% of China's total installed electric capacity. 16,8% of German electricity consumption comes from a renewable source. [Ren]

1.1.2 PV development, potential

The PV industry had an extraordinary year, with global production and markets more than doubling in 2010. An estimated 17GW of capacity was added worldwide (compared to just under 7.3 GW in 2009), bringing the global total to about 40 GW – more than seven times the capacity in place five years earlier. This 40 GW total PV capacity compared to other renewable capacities in 2010 as follows: 1 010 GW of hydro power exists, 198 GW of wind and 185 GW of solar hot water global capacity exists.

Photovoltaic panels were installed in more than 100 countries in 2010. In the past 5 years the annual average growth rate was almost 50%. The thin film share is 13% within PV sector, which is less than the share of the previous year (17%).

In Europe the newly installed 13.2 GW PV is enough to serve 10 million household's electricity consumption. In 2010 Europe added more PV capacity than wind renewable capacity. Germany itself covers one third of total last year PV installation, but also Japan and USA PV market doubled compared to 2009.

There are still large differences between the typical energy costs among the different power generation systems. Costs vary in a wide range, from large hydro 3-5 US cent/ kWh to rooftop PV 17-34 UScent / kWh. PV is still the most costly in term of pure economical calculation and excluding environmental costs (Fucushima, global warming, etc.). After PV the second most "expensive" energy source is offshore wind power with 10-20 UScent / kWh. In rural areas small, household wind turbine electricity production cost of 15-35 UScent / kWh comparable to rooftop PV.

In the last year after wind (90 billion USD) photovoltaic had the second largest utility-scale asset finance sector with a 19 billion USD investment. This was higher than investment in 2009 but below the 2008 record of 23 billion USD.

Thin film production increased in 2011 by a record of 63% and it was 3,2 GW. The location of production continued to be concentrated in Asia: while in 2009 50% and 2010 59 % of total production came from China and Taiwan, in 1st quarter 2011 85% of total production took place in Asia. North America produced 13% of total production and had a large part of thin film production, with half of thin film produced there.

PV Cycle established the recycling network for end of life PVs in Europe. By March 2011 150 tons of PVs were collected and it is estimated that just in Europe 130 000 tons of end of life panels needed to be collected by 2030.

After the bio fuel and wind power industries, solar PV was the third largest provider of employment within renewables. In Germany alone the PV industry provided employment for

120 000 employees. [Ren]

1.2 Core objective

1.2.1 Live productivity of second generation PVs

In the 21st century second generation photovoltaic cells development considers not only the absolute highest power output of photovoltaic cells but also takes into account the ecological and economical production cost.

The absolute highest sunlight induced electricity power production efficiency in research phase is over 40%. [Nrel] This result is reached by multi junction concentrators. In applied daily practice the second generation PV model's price, economical feasibility and partly also the ecological load are the major factors.

The first generation photovoltaic crystalline silicon cells have up to 20% efficiency. The production cost includes the energy consumption of ingot production on 800-1000 °C and losses of high purity ingots / wafer during the sawing process, both of which have a negative influence.

The second generation photovoltaic cells are developed using a much cheaper, less energy consuming silicon-based technology. The production temperature is around 200 °C, there are no sawing losses and the layer thickness is at most some tens nanometers in the case of amorphous, protocrystalline and microcrystalline silicon cells. The power production, and thus the efficiency of these second generation PVs, is limited by about 8-12%. The SWE phenomenon, which is a key efficiency limitation, is still not yet fully understood. Only empirical data described the degradation and also there is the not totally understood seasonal panel temperature dependent alternating power production of no crystalline silicon based PV's.

1.2.2 The target of this thesis

As amorphous silicon based PV commercial usage becomes more and more common, it is important for consumers and also for the implementation companies to know the real degradation time and percentage in practice.

Regarding the literature there are some additional questions. The literature used to categorize amorphous silicon based cells as a PV device for hot, rural areas. as it is cheap and has increased production in the summer while crystalline silicon has losses in the summer. It would be very interesting to see if under Central and Eastern European conditions

Master Thesis

MSc Program
Renewable Energy in Central & Eastern Europe

there was any degradation and seasonal fluctuation differences if the panel was in a more highly irradiated portion of the roof (e.g. south) or a less highly irradiated portion of the roof (e.g. west or east).

The core objective of this thesis is to develop a reliable method for the measurement of real productivity and degradation of newly developed micromorph photovoltaics and for heterojunction amorphous contain photovoltaics. Economic comparisons could also be made from the real productivity.

1.2.3 Method of measurement development

In this thesis we are practically measuring some recently implemented thin film applications and their degradation. As degradation and concrete performance depend on the period of exposure, temperature of the given panel, and temperature fluctuation, we attempted to make comparative measurements under different circumstances, at different locations with different roof orientation and inclination.

The basic method is to compare the real early stage productivity of different thin PVs with the assumed stabilized productivity. From these data we will present, compare and discuss the real productivity of the newest hetero-junction amorphous-crystalline contain and mycromorph PVs and check the applicability of the method.

1.3 Citation of main literature

1.3.1 Basis of photovoltaic electricity production

The photovoltaic effect first was released by A.E. Becquerel in 1839. Albert Einstein described the photovoltaic effect and he received the Nobel Prize in Physics for it in 1921. [WikLc]

As photon (light) reaches a direct semiconductor electron, and the energy of the photon is greater than needed to overcome from the valence band to the conduction band, the electron of the direct semiconductor is lifted to conduction band. In this status of semiconductor the electrons on the conduction band are in excess. [FGC, p122]

Free electrons are shared among all the atoms of the solid and are not associated with any particular atom. They are very mobile.

As electrons on the conduction band are allowed to flow through the semiconductor, an electric field can create an electric current and produce electricity.

When in a semiconductor the electron “jumps” to the conduction band a “hole” remains on

Master Thesis

MSc Program
Renewable Energy in Central & Eastern Europe

the valence band. This means electrons move in one direction and holes move in the opposite direction. The **electron-hole pair** flow generates the current.

This flow or electron-hole transport can be either drift or diffusion movement, depending on the type of force driving it. Electric field driven movement is called drift, while a density and gradients forced process is called diffusion movement. [FGC]

Electricity- creation

When the energy of light makes contact with the n-type semiconductor, an electron-hole pair is generated. The number of holes (minority carrier concentrations in n-type) are significantly increased. This changes creates the concentration-electrostatic balance. [Bur, p7-8] Electron flow starts in the direction of n-type material and holes in the opposite direction. The electric-hole flow is collected in the p and also on the n type side. The p-type semiconductor faces the sunlight where a metal grid collects the electron flow, while on the p-type back side is a solid metal. [FGC, p122-123] In this manner the p-n semiconductor junction creates DC (direct current) electricity using energy caught from the photon.

1.3.2 Types of silicon PVs

By adjusting the band gap, the producer can determinate which energy level of absorbed light it is willing to use for electricity production. Infrared has 0,5 eV while ultraviolet has 2,9 eV energy. In the visible spectrum red light has 1,7 eV and blue light has 2,7 eV. As described in Annexis (7.2. Definition of some photovoltaic terminology, Doping), intrinsic crystalline silicon has a 1,12 eV band gap. To capture as much of the energy of the light as possible, the whole spectrum of arriving energy should be used. As a certain adjusted semiconductor has a given band gap, a huge amount of caught sunlight energy is either below its band gap or carries excess energy. To improve efficiency many types of solutions and combinations of these solutions are applied in silicon based PVs.

For example, one can lay two or more p-n semiconductors with different band gaps in order to permit the capture of different energy content photons. In this manner a wider energy range can be converted to electricity. Photons with high energy in the blue range are used in the most topmost, widest band gap semiconductor, while red light photons with lower energy content provide sufficient energy for electrons to get from valence band to conduction band in the bottom layer.

Types of silicon PVs according to the crystalline and crystal size

The structure of the material also predicts the efficiency of the semiconductor. There are three types of silicon used for PV solar cells: crystalline, polycrystalline and amorphous silicon. [FGC, p129]

Crystal silicon (also called: single-crystal, monocrystal; abbreviation: c-Si): the silicon atoms are in pure crystal order. All silicon atoms have four covalent bonds to their neighbor four silicons. All bonds have the same length and the same angles between the bonds. For the process of c-Si semiconductor required impurity content must be below 10^{-9} . Crystal silicon wafers are made of cylindrical ingots with cutting techniques. The c-Si has high conductivity as there is theoretically no fault (e.g. dislocations, twins, stacking) in the structure. C-Si has the highest efficiency which is about 15-20 %. [FGC, p129]

Polycrystalline/microcrystalline (multicrystalline, abbreviation: poly-Si or μ c-Si): polycrystalline made of various silicon crystals. In poly-Si ingots smaller crystalline parts are together, and various silicon crystals forms an ingot. Poly-Si wafers are also made of ingots with cutting techniques. The poly-Si has faults in the structure. The conductivity of poly-Si is lower than of c-Si. Microcrystalline is made by vapor deposition. The development is described in the next chapter.

Ribbon silicon is a type of multicrystalline. It is not sliced from ingots but formed by drawing molten silicon. The efficiency of ribbon is smaller than of poly-Si. The production cost is much smaller as silicon waste during sawing is minimized.

Amorphous silicon (abbreviation: a-Si) has no crystal structure of any kind. The silicon atoms are not in ordered covalent bonds, rather, there are many dislocations, twins and stacking "faults" in compared crystalline. There are so called larger deviations in bonding length and angles. In this case weak bonds can be easily broken by sufficient outside energy. There are atoms with too many or too few bonds. When a silicon atom has only three covalent bonds to the neighbors and has an unpaired bond, it is called a dangling bond. In a pure a-Si:H the concentration of dangling bonds is $10^{21}/\text{cm}^3$. In hydrogen alloy the hydrogen forms a strong bond to the dangling bonds and the defect concentration decreases to $10^{15} / \text{cm}^3$. The a-Si has the lowest conductivity and the lowest conversion efficiency (7-12%) among the three forms.

Protocrystalline is defined as being fully amorphous. It is also produced with chemical vapor deposition but when the hydrogen-to-silane ratio is lower in the reaction gas than the

Master Thesis

MSc Program
Renewable Energy in Central & Eastern Europe

amorphous end material has “enhanced medium-range order” [AIM, p3]. Protocrystalline has a slightly higher band gap, which means 100-200 meV higher than standard amorphous silicon [Shacell, p240].

The assembly of amorphous silicon PV is different than crystalline silicon. Because of the amorphous structure the carrier lifetime is shorter and the carrier mobility is lower than in crystalline silicon. Therefore in amorphous silicon a drift zone is included to increase the carrier collection. [PA, pxxii] In amorphous cells between p and n semiconductor layer an **intrinsic layer** is installed. Intrinsic layer is not doped with any “foreign” atom [KSW, p250]. This region is the absorber region and ensures that in electron and hole reparation, the electric field created by n-p layers extends all over the intrinsic layers.

The main differences of a-Si:H and $\mu\text{c-Si:H}$ are:

- The band gap of $\mu\text{c-Si:H}$ is close to c-Si:H, around 1,1 eV.
- Because of crystalline nature of $\mu\text{c-Si:H}$, its indirect band gap results in weaker absorption values than those of the direct band gap a-Si:H.
- The light induced degradation effect is either non-existent or exists in a much milder form in $\mu\text{c-Si:H}$ relative to a-Si:H. [PA, p149]

1.3.3 Efficiency

The efficiency of the layer is calculated by dividing useful power output (electricity created) by the total that arrived to the surface of the cell (power of light hitting the cell’s surface).

Theoretically the highest efficiency can be reached with a material with a band gap equal to the highest power portion of the overall spectrum.

The solar spectrum arriving to the Earth can be approximated by the black body of 5900 K. Figure 4 shows the black-body, air-mass 1,5 and air-mass 0 efficiency limit in term of different band-gap between 0,5-2,5 eV. As seen in Figure 2, that the material with one band gap should chose which is the band gap that can convert the highest amount of solar energy from the arriving spectrum. It is also seen that crystalline silicon did not reach the highest efficiency band gap, as even amorphous silicon has higher efficiency.

Master Thesis

MSc Program
Renewable Energy in Central & Eastern Europe

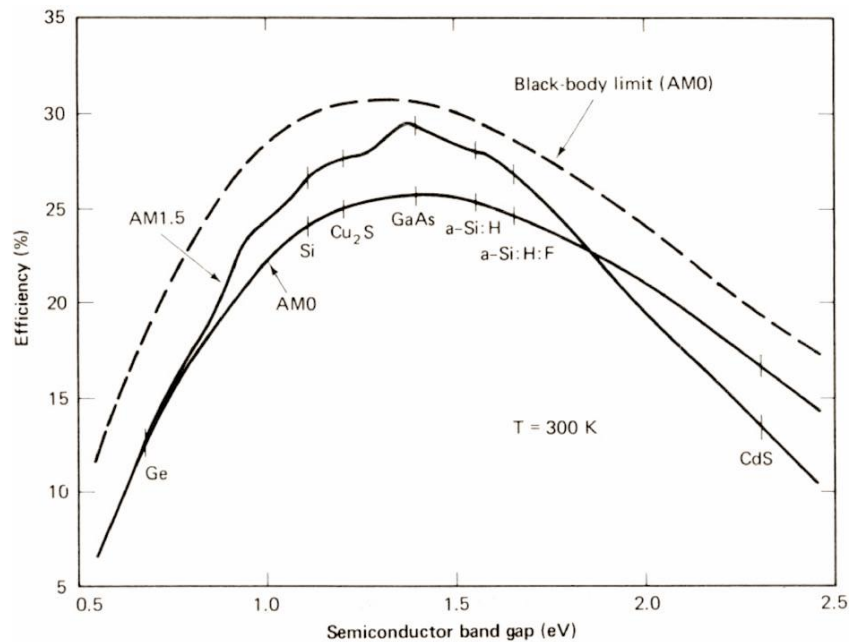


Figure 2: Conversion efficiency of different band gap semiconductors. The band gap of amorphous silicon fits the solar spectrum better than that of crystalline silicon [SD, p1].

The stabilized cell laboratory efficiency for amorphous silicon is around 13%, module efficiency is 6-8%.

For a single solar cell efficiency depends on what percentage of the arriving energy fits to the band gap. The photons which have less energy content than the band gap will not generate electricity, therefore the excess energy content photons will be lost.

In a single cell the relative spectrum efficiency can approach 100%. Relative spectrum efficiency describes the given spectrum conversation efficiency and not the whole spectrum compared to the transformed energy.

Degradation

Efficiency degradation first was reported by Stabler-Wronsky more than 40 years ago, in 1977, and since then has been called the “Stabler-Wronsky effect” (SWE). Since then the SWE has not been fully understood.

Due to degradation the short circuit current and FF decrease and the open-circuit voltage remains almost constant.

In amorphous silicon the level of dangling bond density is extremely high, more than 10^{19} - 10^{21} / cm^3 . The degradation of a-Si is much higher than of hydrogen diluted a-Si:H as

Master Thesis

MSc Program
Renewable Energy in Central & Eastern Europe

hydrogen makes many of the dangling bonds passive. [PA, pXX] The dangling bond density of hydrogen diluted a-Si:H reduces the intrap state density to $10^{15} / \text{cm}^3$. Even then the efficiency loss of a-Si:H can be as high as 15-30% of original power output. The $\mu\text{c-Si:H}$ have better stability than an a-Si:H or a SiGe:H solar cell. [RD, p618] The stability of a-Si:H/ $\mu\text{c-Si:H}$ is still questionable, and experimental data is needed [ZB, p9]. Light induced defects depend on many deposition conditions.

There are many explanations of light induced degradation, but until now it has not been fully understood.

- The stability of the cell is related to the hydrogen content. The electron carriers breaks the weak silicon-hydrogen bonds, which means additional defects occur and the defects increase in the serial resistance [44, p61]. Other authors mention defects like increasing the density of the dangling bands. [WRK, p1148]

Thus, the system is driven into an excited higher energy state, with active defect centers leading to higher recombination of the free carriers and hence a reduction of efficiency. [Raz, c4.4.3.1] In other words *the metastable Si dangling bonds increase and the density of mid-bandgap states increases. The number of metastable states is limited thus degradation due to LID is limited* [RD, p618]

- Another explanation of metastable defects-caused degradation is that the metastable defect acts as an extra trap. The result of trapping is that the electric field across the intrinsic layer is distorted and the space charge distribution in the intrinsic layer deflates. Lower drift, lower carrier collection. [PA, p212]
- A different means of creating additional dangling bonds is described by the Hydrogen collision model. It is assumed that *the incoming photon or an injected charge carrier releases a hydrogen atom from a Si-H bond. The H atom diffuses through the network. If two diffusing hydrogen atoms open a weak Si-Si bond and from two Si-H bonds, the original sites that these hydrogen atoms left behind remain dangling bonds.* [WCB, pc4]

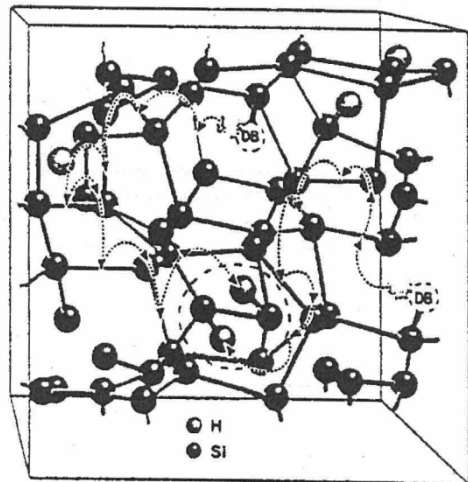


Figure 3: Hydrogen collision model assumes that degradation is caused by loose hydrogen atoms, which can open a weak silicon-silicon bond.

- Foreign atmospheric impurities like carbon, nitrogen and oxygen also have correspondence to light induced degradation.

An empirical approach led to reduction in SWE by optimizing the growth conditions to improve the microstructure. [WRK, p1148]

The light-induced degradation of the top amorphous cell can be minimized by keeping its thickness small. This determines the amount of generated current in the whole cell. [ZB, p6] Increasing the I layer's thickness can increase I_{sc} (short circuit current) but reduce U_{oc} (open circuit voltage) and FF (fill factor) (see Annexes definitions). [ZB, p11] An I layer thickness over 300 nm in a single solar cell would boost the degradation, which in this case could be as high as 20-40%. [ZB, p9]

Empirical studies have shown that bottom cell limited a-Si:H/ μ -Si:H stability is better than top cell limited. And there are also results showing that a mismatched or relatively large initial current difference ($I_{sc} > 0,8 \text{ mA/cm}^2$) between the top and bottom double junction has smaller SWE than cells with matched layers. [ZB, p10]

2 Description of method of approach applied

2.1 Elements of method

The basis of the method is to determine critical points of the live production measurement of amorphous silicon systems. The most important aspects of initial data collection were:

Master Thesis

MSc Program
Renewable Energy in Central & Eastern Europe

- first production data obtained as soon after installation as possible
- systems should be relative large in size (40-50 m²) compared to laboratory quality test areas (1-5 m²)
- reliable data: should attempt to ignore any external influencing circumstances, such as a very variable irradiation day when the irradiation versus production and panel temperature are very unstable
- data collection from operating installed systems
- development of a calculation method which can be used for different panels
- development of a calculation method which makes the results comparable
- different locations with different seasonal irradiation amount and intensity, as well as different seasonal average daily temperatures.

The method was planned to conduct empirical tests, and from these test results to make production, degradation and economical comparisons.

2.2 Data of producers

There are approximately some tens cell producers and approximately some hundred photovoltaic panel producers worldwide. Panel producers' advertisements (brochures and web) generally show their costumers the peak load power production of the panel, the size of the panel (length, width, height, etc.), the structure of the panel (e.g. thermally strengthened front glass, PVB or EVA foil, thermally strengthened rear glass), and also some information about the cell. In some cases the information given about the structure is very limited (e.g. amorphous and microcrystalline silicon, multi junction cell), while sometimes it includes the cell structure. Sanyo for example provides a diagram with basic, educational lecture data about the cell structure and the mechanism of the cell (Figure 4).

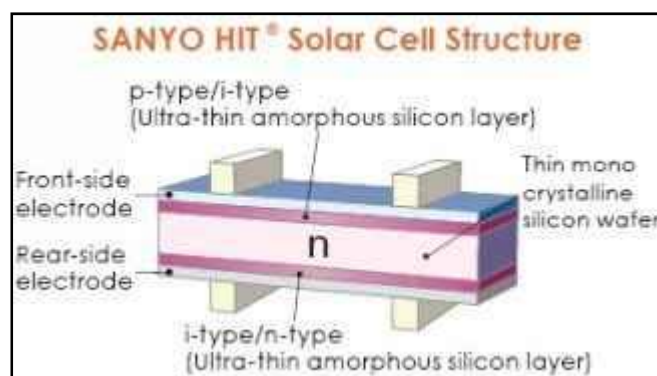


Figure 4: Sanyo HIT cell heterojunction structure. Mono crystalline silicon is combined with n and p type amorphous silicons.

Master Thesis

MSc Program
Renewable Energy in Central & Eastern Europe

The maximum power output or peak performance is often called nominal output. This value indicates the performance of a solar module under full sun exposure and is defined under testing conditions. It is based on measurements taken under optimal conditions.

In case of amorphous or hetero / multi junction cells the producers also give the power production (I_{mpp} and U_{mpp}) percentage decline interdependently from the sun irradiation intensity. The performance of PV's also depends on the cell temperature. The thermal characteristics are normally given.

Introduction of applied panels

In this measurement method development two types of multi-junction tandem cells were used. Bosch μ -Si plus 115, which is a micromorph (amorphous/microcrystalline) tandem cell, and Sanyo HIT, which is a multi-junction cell where the mono crystalline silicon wafer was combined with a thin amorphous silicon layer.

The advantage of multi-junction is to combine different band gaps so the incoming light is used more efficiently. This is also the basis of micromorph cells. During the production of micromorph cells manufacturers do not need to use toxic materials like germanium to develop different band gap layers. The band gap combination of 1,1 eV for the bottom cell microcrystalline and 1,7 eV for the top cell amorphous cell uses light more effectively.

In this manner it is also possible to use thinner amorphous top cell and reduce degradation. The third advantage is the possibility of obtaining higher U_{oc} and lower I_{sc} , which leads to reduction of electrical resistance.

The μ -Si:H has an indirect band gap while a-Si:H has direct band gap, which means the relatively absorption coefficient of the two different layer differs significantly. Thus, in a micromorph tandem cell the microcrystalline bottom cell needs to be much thicker than the top amorphous layer. [PA, p160-161].

In laboratory scale the initial efficiency of micromorph cells is over 14%, and the stabilized efficiency is 11-12%. This study will show how they perform in some in situ cases.

In the calculations we used producers' data provided by Sanyo and Bosch as shown in Figure 5 and listed in the calculation chapter 2.4.

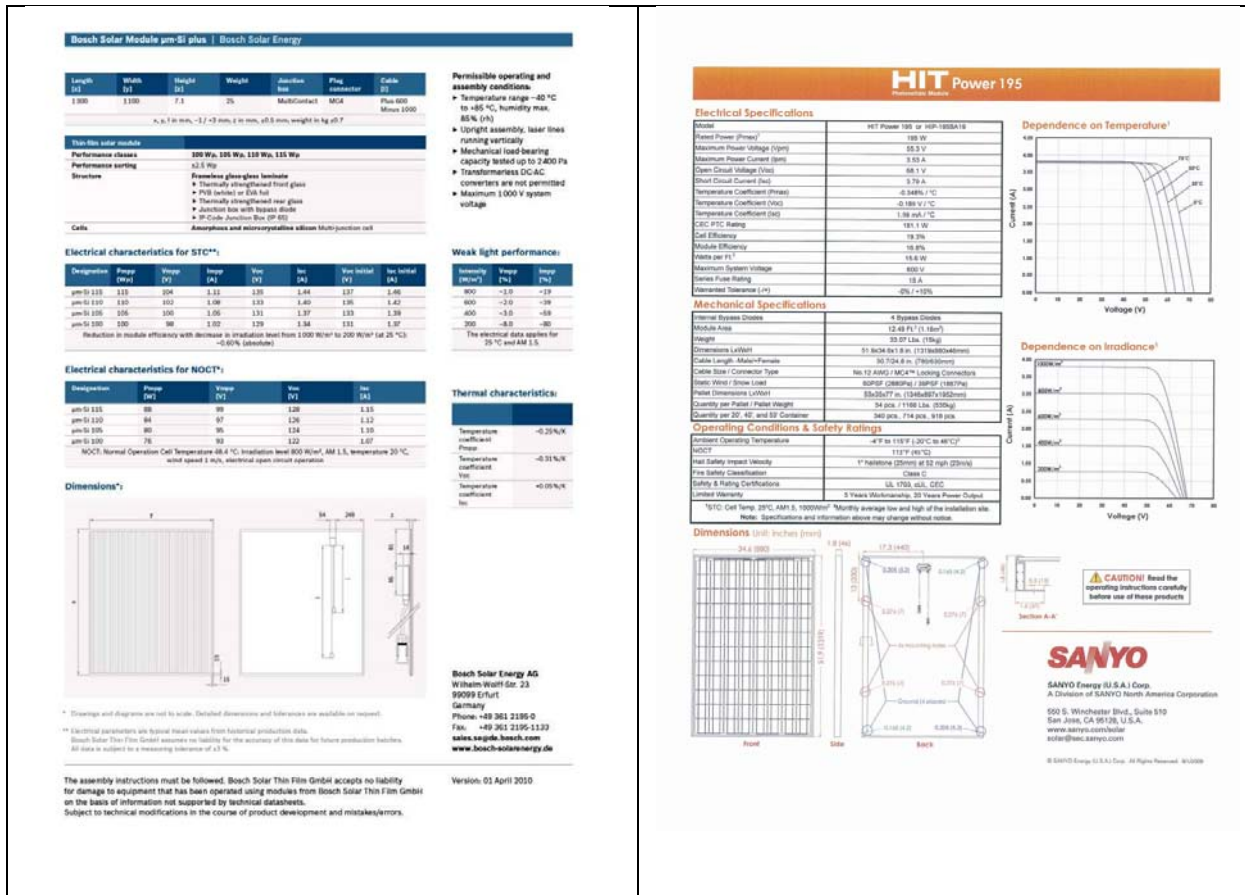


Figure 5: Data sheets of Bosch μm-Si plus 115 and Sanyo HIT Power 195

2.3 Expectations based on relevant literature

2.3.1 Productivity and efficiency

The panel productivity printed on sales leaflets is a number measured under Standard Test Conditions. Definitions of Standard Test Conditions (STC) can be found in the Annexes.

It is difficult to describe the productivity of different types of solar panels such as crystalline based and thin film solar panels. The most commonly used method to characterize different cells is the conversion efficiency. First Solar, the world's leader thin-film solar manufacturer, reached an average cell efficiency of 10.6 percent in 2007. The most efficient commercially available silicon-based cell producer, SunPower Corporation, manufactures and sells panels with 22-percent efficiency.

The question is: does the peak efficiency of the solar panel describe well the capacity of the panel well? Will the customer get full information if he compares the peak efficiency of different panels?

Master Thesis

MSc Program
Renewable Energy in Central & Eastern Europe

Thin film panels produce more electricity than crystalline panels in real life conditions, even though the efficiency number makes it look like they produce less.

There are two major reasons.

- First, traditional crystalline panels' thermal characteristics show a higher negative temperature coefficient, as they become less efficient when they heat up than thin films, which lose less efficiency at higher temperatures. This is because crystalline silicon solar cells have a band gap of 1,1 eV with a temperature coefficient which is about twice the temperature coefficient of amorphous silicon solar cells with much higher bandgap (1,7-1,8 eV). The relative drop in the efficiency of c-Si is about -0,5%/K, while this value is only -0,20 %/K for amorphous Si. Microcrystalline solar cells have temperature coefficient somewhere between that of crystalline and amorphous cells. [Shacell, p248]
- Second reason is that amorphous silicon solar panels have higher quantum efficiency in lower wave lengths (0,5-0,6 μm), while crystalline silicon optimal spectrum intensity is at higher (0,8-1,0 μm) wave lengths. This advantage is important in areas like Central Europe, where there are approximately 1 000 sunny hours a year and many cloudy days. Thin films can make electricity in diffuse light, while regular silicon-based panels need more direct light. This can mean that for certain consumers (e.g. in Central Europe), thin films can produce more electricity throughout the day than crystalline.

As a final conclusion thin film technologies might deliver the same or higher cost per watt than a monocrystalline panel, but a lower cost per kilowatt-hour.

This is why the simple peak power efficiency is not the best information for consumers, but thin film retailers have not yet found a better comparative number. [Giga]

There is a third factor that makes the comparison of degradation complicated. There is not yet a standardized test method of describing degradation. The degradation test, often called light soaking test in Japan, is the value after 310 hours under 1,23 sun equivalent light intensity, 48 °C temperature and open circuit conditions. In the USA the stabilized efficiency is the value after 600 hours under 1 sun equivalent (= 1 000 W/m^2 solar irradiance) at 50 °C on open circuit conditions.

There are also many other effects that determine theoretical cell efficiencies:

Master Thesis

MSc Program
Renewable Energy in Central & Eastern Europe

- A part of the light hitting the upside of the cell can be reflected back by the conducting grid system.
- Reflection losses when radiation is transmitted from air to the cell. To reduce such losses cells have structured surfaces and anti reflective coatings.
- Short-wavelength penetration not as deep as long-wavelength. Charge carriers tend to re-combine very quickly before they involve contribution of processing photocurrent.
- Impurities and imperfections in the silicon where carriers tend to recombine, too. The impurity must not exceed 10^{-9} .
- The surface of crystalline silicon is also an imperfection. There are various techniques to reduce this efficiency loss.
- Short circuit between front and rear side is typically a manufacturing fault.
- There are many losses during transmission of energy, like resistance losses. [KSW, p242-243]

There is also another indicator that serves as an index for the quality of the photovoltaic cell. This is the relation between the maximum power (maximum current and maximum voltage), and the “measured” maximum power (open circuit voltage times short circuit current). This relation is referred as Fill Factor (FF). When the measured power is closed to the maximum power the FF is close to 1, while when there is larger difference, FF is less. FF is defined in the annexes. [KSW, p242-243]

The literature about efficiency describes the research results and the commercially available panels’ efficiencies, too.

Research results discuss new top technology efficiencies of some square millimeter size panels. The efficiency development of solar panels is shown in Figure 6, which indicates the crystalline silicon cells’ thin film technologies, concentrators and the different novel PVs. Efficiency development is not always harmonized with economical feasibility.

Master Thesis

MSc Program
Renewable Energy in Central & Eastern Europe

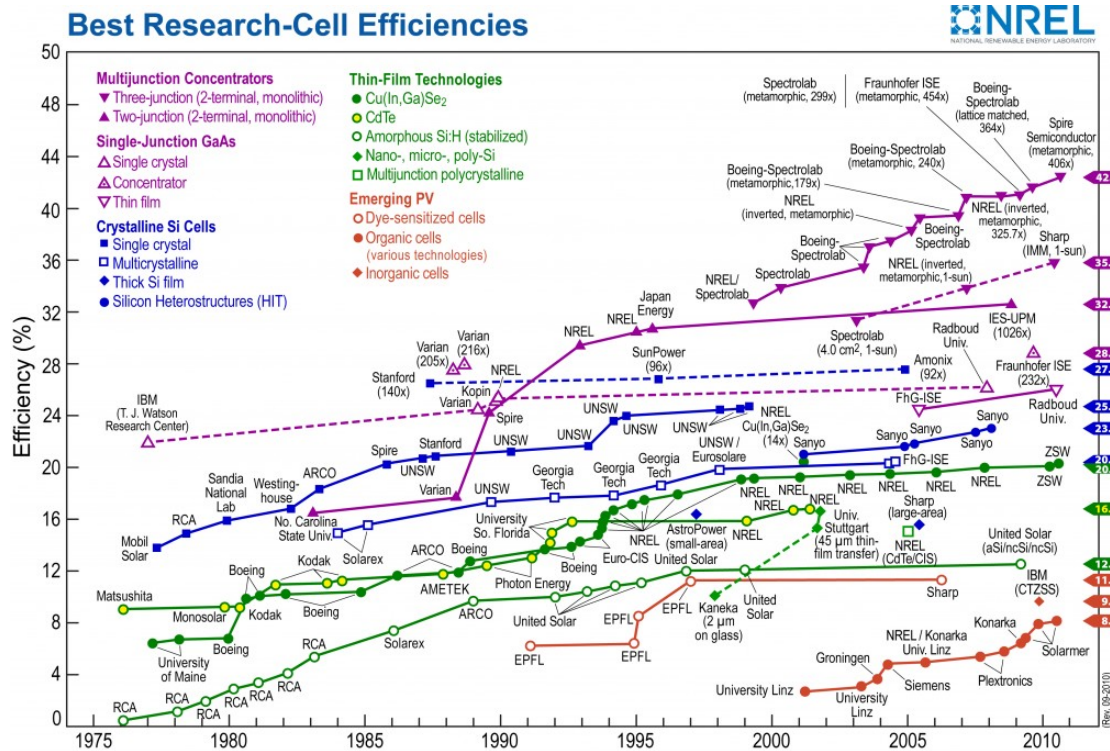


Figure 6: Best research PV cell efficiencies of different type of cells [Nrel]

Table 1 shows the difference in efficiency measured under laboratory conditions and what could be implemented under a manufacturing size production scale. Table 1 shows that industrial scale produced panels are less efficient than the published research phase panels.

Master Thesis

MSc Program
Renewable Energy in Central & Eastern Europe

Table 1: Top efficiency of different type solar cells (only cells listed with larger surface than 1 cm² have been considered) [KSW, p244]

Material	Type	Efficiency, %		State of technology
		Laboratory	Manufacturing	
Silicon	monocrystalline	24,7	14,0-21,5*	large scale production
Polysilicon, simple	polycrystalline	19,8	13,0-15,5	large scale production
MIS inversion layer (silicon)	monocrystalline	17,9	16,0	small scale production
Concentrator solar cell (silicon)	monocrystalline	26,8	25,0	small scale production
Silicon on glass substrate	transfer technol.	16,6	-	pilot production
Amorphous silicon, simple	thin film	13,0	8,0	large scale production
Tandem 2 layer, amorphous silicon	thin film	13,0	8,8	small scale production
Tandem 3 layer, amorphous silicon	thin film	14,6	10,4	large scale production
Gallium indium phosphate / gallium arsenide	tandem cell	30,3	21,0	small scale production
Cadmium-telluride	thin film	16,5	10,7 – 17,3	large scale production**
Copper indium di-selenium	thin film	18,4	12,0	small scale production

* SunPower, Sanyo, etc., ** [Ren]

2.3.2 Expectations of degradation curve

There are ample empirical data on different cells' light induced degradation from research and large scale PV implementation.

The stabilized performance of high quality hydrogenated amorphous silicon cells is 70% to 85% of their initial performance. [PA, p211]

Efficiency degradation in practice depends not only on the degradation described by the Stabler-Wronsky Effect, but also on many other factors influencing the amount of power generated. In an outdoor test of photovoltaic arrays in the Saharan region in Algeria, the following two main factors caused degradation:

Master Thesis

MSc Program
Renewable Energy in Central & Eastern Europe

- discoloration of the EVA copolymer encapsulant: browning of the of the encapsulant in some areas in the inside modules. This browning often happens, after long term exposure to UV sunlight with module temperature near 50 °C.
- hot spots can occur due to many formations of cell failure: interconnection failure, partial shading, mismatches, inadequate module bypass, or a cracked cell in the module.

In the real practice in the desert two other major problems occurred:

- due to the thermal differences the module wiring connectors slackened off
- dust in the electrical connection boxes caused bad connections.

All long term monitoring programs show a saturation of the degradation effect, at the latest after two years of operation. [KSW, p251]

In a 14 month long photovoltaic performance test in Port Elizabeth, South Africa three commercial amorphous silicon modules were tested. A rapid initial power output decrease was observed in all three modules. The initial rapid decrease in peak power output occurred in the first 200 sun hours (approximately 4 weeks) of being in direct sun, and then the future decrease occurred more slowly. This is because the number of metastable dangling bonds is limited. In this test the decrease of single junction modules was around 25%, and the decrease of triple junction modules was 10%-15% in the first month. In this test under the South African climate some regeneration, even incremental efficiency could be detected in the summer months due to annealing. In the colder winter months the degradation again became more intensive. The degradation and regeneration were competing during the seasons. [RD, p620]

In general we can say the (hydrogenated) amorphous thin film efficiency degradation process occurs in the initial couple of months of exposure to sun, and extends to maximum two years. Some authors are highlighting *the light induced degradation occurs rapidly in the first 48 hours after exposure to sunlight, and then degradation saturates, decreasing the rate of degradation. [RD, p618].*

The degradation rate is **not affected by interruption**. A dark period within the sun explosion (degradation process) does not illuminate the earlier efficiency state of the cell. Once the cell is illuminated again the photoconductivity will drop from the rate before dark period. [WikSW, p1]

Master Thesis

MSc Program
Renewable Energy in Central & Eastern Europe

The degradation is **reversible** by exposure to temperature around 150-160 °C. The heating recovery depends on the temperature of the cells; for instance, annealing at 70 °C helps to stabilize the system better than at room temperature. [Raz, c4.4.3.1] **Seasonal efficiency changes** also detected: in winter the efficiency drops and recovers during summer due to annealing. Output power in winter decreases with 70% of the initial value and in the summer can reach again 80% of the original one [RD, p618].

Other authors discussing the following causes for summer month regeneration: spectral effects, thermal annealing or light-induced annealing. [RD, p617-618]

Regeneration and degradation are additive, resulting in an overall slower rate of degradation.

Long term peak power degradation is typically composed of three factors as shown in the idealized curve in Fig 7. The first is the degradation on “stabilized” curve (curve A). This is the initial degradation seen in the first year (Staebler-Wronsky effect). Most of the decline is actually seen in the first month or so and asymptotically approaches a “stabilized” P_{max} value ideally equal to the module rated P_{max} value. The seasonal variation of some 5% to 8% is seen with the P_{max} cycling around the stabilized P_{max} value (sine curve B). Superimposed upon this seasonal cycle is a gradual long-term degradation, typically of some 0,5% to 1% for the life spam of the module (straight line C). ... Most studies ... suggest that the long-term degradation of c-Si or pc-Si and that of a-Si are fairly comparable. [Osbr, p3-4]

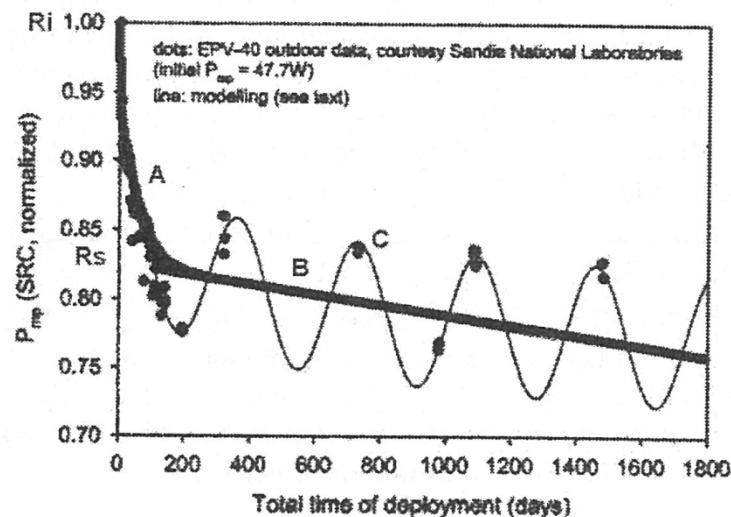
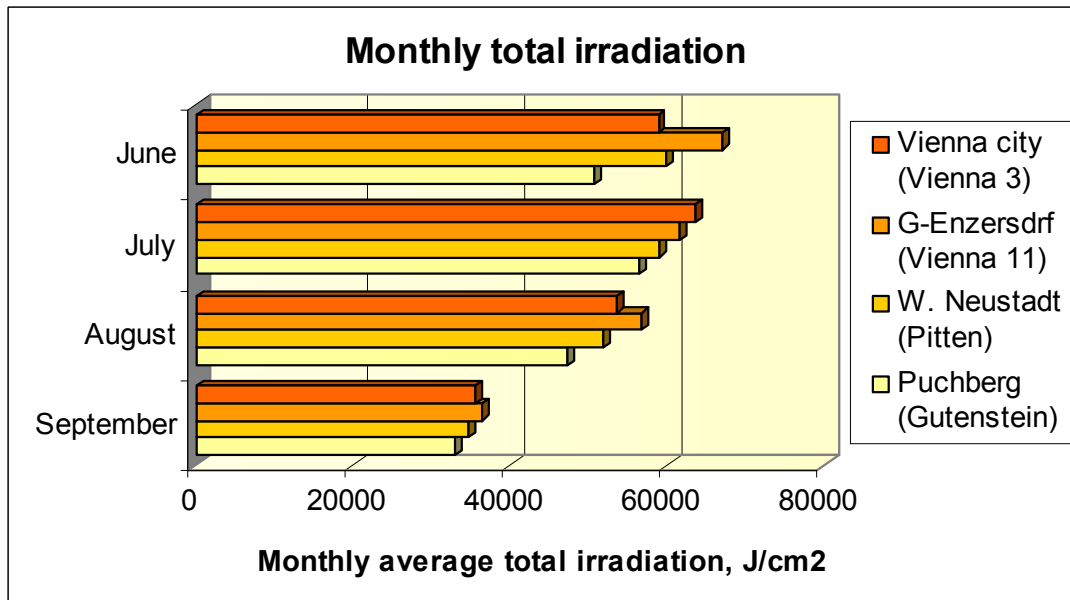
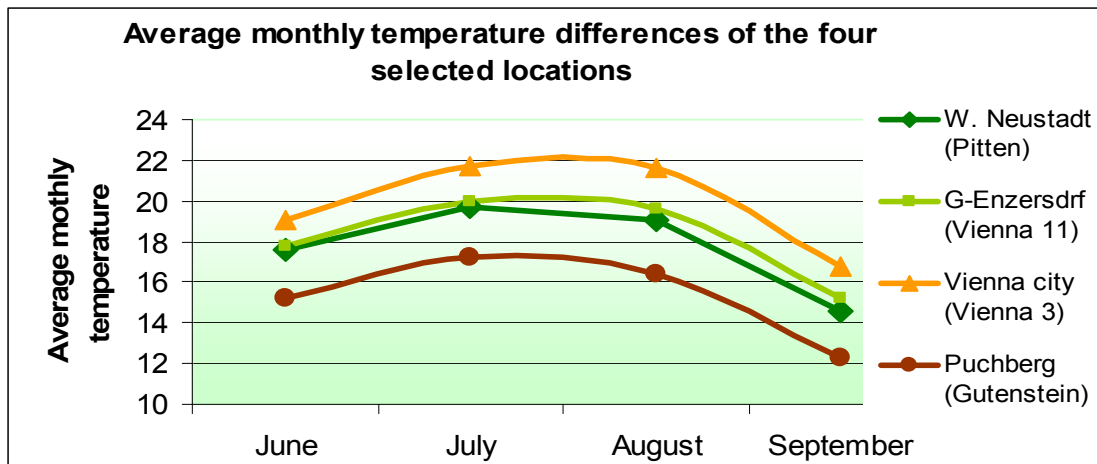


Figure 7: Seasonal efficiency alternation of amorphous silicon PVs: degradation and regeneration of single junction (Si-1) and triple junction (Si-2 and Si-3) amorphous silicon solar cells in South Africa. Section A: first month of sun explosion, Section B and D: colder winter period, Section C and E warmer summer period. [RD, p620]

Master Thesis

MSc Program
Renewable Energy in Central & Eastern Europe

As shown by the literature mentioned above, degradation depends on the time duration of expose to sun and the seasonal temperature. Therefore, different degradation intensities were expected from different locations. Measurement sites were selected to obtain locations with relatively large weather differences. The weather characteristics of the locations are presented in the Figure 8 and chapter 7.1.



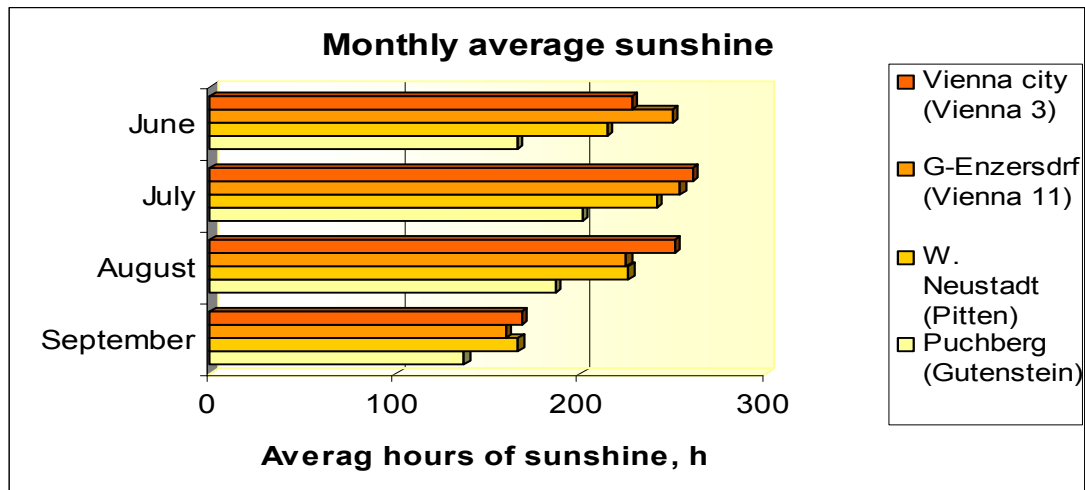


Figure 8: Even the selected four test locations are in a 60 km circle distance they have a strong average temperature, irradiation and sunshine hours difference. [ZAM]

It is shown that the August total amount of sunshine hours in Gutenstein is almost 35 % less than in Vienna city. Also, the June-September daily average temperature is more than 5°C less in Gutenstein and the August total irradiation in J/cm^2 is more than 20 % less than in the capital city. This is a good basis for comparing degradation intensity under different circumstances.

2.4 Targets of measurements

The main targets of our measurements in order of importance were as follows:

- first of all to find the main critical points of an in situ, not reproducible measurement which has many external influential coefficients
- to determine the real efficiency degradation of amorphous, microcrystalline (micromorph) solar cells maintained in a mild climate (Central Europe) by an entity that had a regular daily practice of PV installation
- to study the real efficiency differences between amorphous / microcrystalline (micromorph) and heterojunction PVs
- to compare the producers' data with actual results
- to see the dynamic of efficiency degradation in different locations (ambient/panel temperature, panel sitting, etc.)
- to study the economical profitability of amorphous / microcrystalline (micromorph) and heterojunction PVs in CEE.

2.5 Calculation of light induced degradation

Efficiency is defined as the ratio between the useful energy produced the panel and the total energy hitting the panel.

As power is the rate of energy, efficiency can be measured as rate between the power that hits the panel and electricity power that comes out of the panel. Electricity power defined as:

$$P = U \cdot I \quad (1)$$

where

P is the power, measured in watt, W

U is the potential difference, V

I is the rate of flow, current, A

To achieve the targets listed above, the sunlight power input and the electricity power output was measured.

The calculation of light induced degradation is built on the measurement of generated power at the mounting phase and measured later on.

The ratio of measured power production and the granted power production was compared at the installation period and 1 ½ - 3 months after it.

$$\Pi = P_m / P_g \quad (2)$$

Where Π is the ratio between the granted power and the measured power, 1

P_m is the measured power production, W

P_g is the granted power production, W

We tried to take the first measurement right after the installation of the panels. This way the initial, not degraded power output could be measured.

The second time the light induced degradation power output of the panels was measured was after 1 ½ - 3 summer months exposure to sun. In the second time we tried to exclude all non light induced power output degradations, like shadowing, dust, electrical failures, etc.

In both cases power generation was calculated from the equivalent (1), which was measured from the following data:

Master Thesis

MSc Program
Renewable Energy in Central & Eastern Europe

- Irradiation intensity on panel surface (ϕ), W/m^2
- Panel surface temperature (T), $^{\circ}C$

- Operating voltage (U_{mpp}), V
- Operating current (I_{mpp}), A

- (Short circuit current (I_{sc}), A
- Open circuit voltage (U_{oc}), V)

- Power DC in, W
- Power AC out, W

The Irradiation on panel surface gave the actual power input of the panel.

The power on Standard Test Condition (STC) output was calculated from the short circuit current and the open circuit voltage by the (3) equation.

$$P_{STC} = U \cdot I \cdot T_c \cdot W_{Lp} \quad (3)$$

Where P_{STC} is the power at STC, W

T_c is Temperature difference coefficient,

W_{Lp} is Weak Light difference performance.

The cell producer provides the following thermal characteristics as temperature coefficient:

$P_{mpp} = -0,25 \text{ \%}/K$ and $V_{oc} -0,31 \text{ \%}/K$, $I_{sc} = +0,25 \text{ \%}/K$ to the STC.

The producer supplied at the STC the current and voltage production of the panel and also given data of weaker light performance. Only four data are given of less light induced voltage and current production: U_{mpp} and I_{mpp} performance losses in percentages. The given data are in Table 2. For the in situ measured power output calculation, one must find the correlation between irradiation and power production. For the voltage drops percentage correlation to the irradiation the following equation fits the best in case of Bosch μm -Si plus 115 (Figure 9):

$$\Delta U_{mpp} = 5,40 \cdot \ln(\phi) - 37,54 \quad (4)$$

Where ΔU_{mpp} is maximum power voltage changes percentage, %

ϕ is Irradiation intensity, W/m^2 .

Master Thesis

MSc Program
Renewable Energy in Central & Eastern Europe

Per Figure 9, the current difference percentage seems to have linear correlation to the irradiance.

$$\Delta I_{mpp} = 0,098 * \varphi - 97,5 \quad (5)$$

Where ΔI_{mpp} is maximum power current changes percentage, %
 φ is Irradiation intensity, W/m^2 .

Table 2: “Weak light performance” data given for the panel Bosch μ -Si plus 115 by the producer.

$\varphi, W/m^2$	$\Delta U_{mpp}, \%$	$\Delta I_{mpp}, \%$
800	-1,5	-19
600	-3,0	-39
400	-5,0	-58
200	-9,0	-78

The electrical data applies for 25°C and AM 1,5.

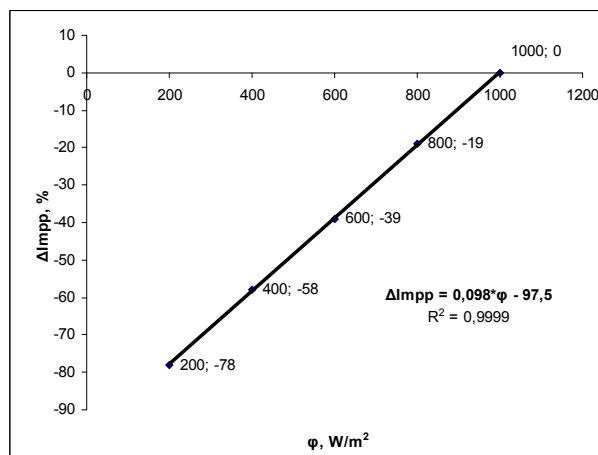
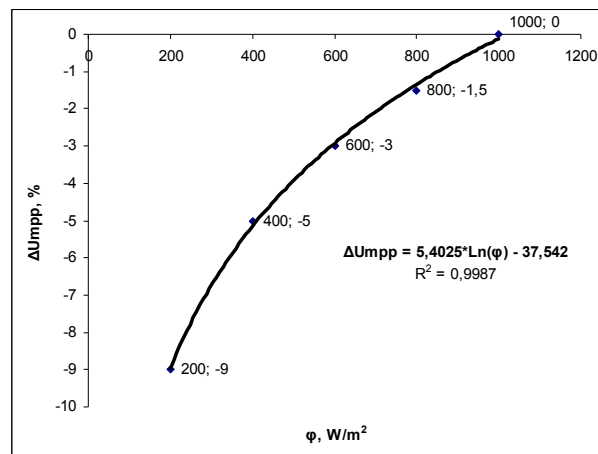


Figure 9: ΔU_{mpp} and ΔI_{mpp} correlation to φ .

Master Thesis

MSc Program
Renewable Energy in Central & Eastern Europe

From the above ΔU_{mpp} and ΔI_{mpp} correlation to ϕ and the equation (3) the producer granted power production of Bosch $\mu\text{-Si}$ plus 115 is

$$P_g = (U_{STC} - (U_{STC} * (5,40 * \ln(\phi) - 37,54) / 100)) * (I_{STC} - (I_{STC} * 0,098 * \phi - 97,5) / 100) * (1 - (T - T_{STC} * 0,25) / 100) \quad (6)$$

Where P_g is producer granted power, W

From the above data actual power production was calculated for granted power of 1m^2 of panel.

The degradation level was identical to the power production difference on initial measured and final measured real production.

2.6 Method of complementary calculation (NPV)

First, this required us to obtain the calculation of key-ready installation of the Sanyo HIT PV panels compared to Bosch $\mu\text{-Si}$. Regarding the installation company, in the following we compare the costs of these two systems in kWp:

	Bosch $\mu\text{-Si}$	Sanyo HIT
Panel cost, €/kWp	1000	1700
Sales cost, €/kWp	1250	2100
Mounting system, €/kWp	450	250
Mounting cost, €/kWp	400	250
Transport cost, €/kWp	100	80
Total cost, €/kWp	2100	2680

As we wanted to make the comparison in situ, the same roof area was theoretically replaced by Sanyo HIT. The theoretically produced electricity of the two different types of panels was compared. The electricity price 0,208 €/kWh, the feed-in-tariff 0,38 €/kWh and the average electricity escalation rate for the coming 20 years was estimated as 2% /annual.

The complementary calculation itself is a Net Present Value calculation:

$$NPV = R_t / (1+i)^t \quad (7)$$

Where t is the time of the cash flow,

i is the discount rate (rate of return that could be earned on an investment in the financial

markets with similar risk.),

R_t - the net cash flow.

3 Documentation of data and data collection

3.1 Description of the in situ measurement

With the advocacy of photovoltaic system planner and installer establishment Nikko-PV, Baden we could participate in four new photovoltaic household system installations in Vienna's 3rd and 11th districts, in Gutenstein and Pitten. All the installations were planned to take place in June 2011. There were many external factors that determined the scheduled implementations, such as panels not distributed in time, bad weather conditions (rain, wind), lack of work force, breakdown of parts (like inverter), etc. Finally two PV systems were completed in the period of June-July 2011.

The system works in Vienna's 11. District. There is also a working system in Niederösterreich, Gutenstein. The locations are within a 60 km diameter circle. Three of the planned locations were in a relatively flat location (150-270 m altitude), while Gutenstein is in a valley on altitude 580 m surrounded by 800-1000 m high hills. The measurements were completed right after the installation, within 24 hours (Figure 10). When the inverter failed the initial measurement was done a week after the panels was exposed to direct sun irradiation. Because of the above mentioned difficulties in determining the exact date of the installation completion at least two days in advance, in the end in two instances the initial measurements was taken by the Nikko-PV company.

Master Thesis

MSc Program
Renewable Energy in Central & Eastern Europe



Figure 10: It was important to make the initial measurement right after the installation. This way we could measure the highest productivity of the panels before the light induced degradation had affected the cells. The pictures show the installation of Bosch μ -Si plus 115 in Gutenstein and the irradiation measurement.

All the measurements were done on not rainy, but in sunny or cloudy days. We tried to avoid the very changeable weather when the irradiation intensity changes very frequently.

Irradiation was measured with solar cell based irradiation meter equipment.

The panel temperature was measured with a laser temperature measurement tool.

All tools used were bought in 2010 with original calibration. Tools and accuracy are listed in Table 3.

The generated current and the voltage of all the installed panels of the given household were measured together just before the inverter. The measurements were achieved by a hand tool digital multimeter. The current was measured by a digital ammeter clamp meter.

Master Thesis

MSc Program
Renewable Energy in Central & Eastern Europe

Table 3: The list and accuracy of the used instruments

Type of instrument	Accuracy
Fluke 177 Series Digital Multimeter, Voltage DC	± (0.09%+2)
Fluke 177 Series Digital Multimeter, Voltage AC	± (1.0%+3)
Fluke 177 Series Digital Multimeter, Current DC	± (1.0%+3)
Fluke 177 Series Digital Multimeter, Current AC	± (1.5%+3)
Voltkraft Infrared thermometer IR 260-8S, 0 °C to 260 °C	± 2 % rdg ± 2 °C
Mencke & Tegtmeyer Si-01TC irradiance meter	± 0.3 %

For Fluke 177 the Accuracies are best accuracies for each function.

The system accuracy is calculated from the absolute accuracy of each system component.

$$\text{System Accuracy} = ((\text{Absolute Accuracy } 1)^2 + (\text{Absolute Accuracy } 2)^2 + (\dots)^2)^{(1/2)} \quad (8)$$

The best power DC system accuracy from the above tool accuracies is 2,71%.

The operating current, operating voltage, and also the generated power DC and inverted power AC were recorded.

All of the Bosch PVs were from the same series of Bosch μ -Si plus 115. This series is an amorphous and microcrystalline, micromorph cell; 100% active surface panel without inactive frame. One panel size is 1 100 * 1 300 mm.

3.2 Data and results of the measurements

Table 4 presents the main data collected in situ after the installation of Bosch panels. As this was the first in situ measurement for us and also for the installation company we had to learn all the details about the process. More data was recorded and two typical examples of each situation are presented.

Master Thesis

MSc Program
Renewable Energy in Central & Eastern Europe

Table 4: The main initial data of in situ measurements

Location	Date of expose to sun/ date of measurement	Sun irradiation, W/m ²	Panel temperature, °C	Impp, A	Umpp, V	Power DC, W	Power AC, W
Vienna, 11 st district	2011.06.23. / 2011.06.28.	540*	28	5,6*	178*	997*	-
		504**		-	-	-	1854
Gutenstein	2011.08.03. / 2011.08.03.	944	52	17,0	234	3978	3697
		951		17,1	226	3864	3718

* one string (18 panels) production data.

** average of three measurements

Table 5 presents the data measured in September after ~45-80 days of sun irradiation to the panels and the calculated relative power production and actual efficiency, which is the partly finished degradation efficiency.

Table 5: Measured data after 1½ - 3 months summer sun degradation panels and its calculated relative productivity and efficiency.

Location	Date of expose to sun/ date of measurement	Sun irradiation, W/m ²	Panel temperature, °C	Impp, A	Umpp, V	Power DC, W	Power AC, W
Vienna, 11 st district	2011.06.23. / 2011.09.12.	252	33,9	-	-	990	934
		297	32,1	-	-	1169	1058
Gutenstein	2011.08.03. / 2011.09.18.	854	43	14,9	229	3412	3100
		876		15,0	225	3375	3195

Table 6 contains the initial and end calculated ratio of granted and measured power P_{AC} and P_{DC} efficiency under STC.

Location	Date of measurement	Ratio of granted and measured power P_{DC} , Π , %	Ratio of granted and measured power P_{AC} , Π , %	Efficiency of P_{DC} η , %
Vienna 11 st initial	2011.06.28.	-	89	-
		90	-	7,2
Vienna, 11 st end	2011.09.12.	96	91	7,6
		96	87	7,6
Gutenstein initial	2011.08.03.	108	100	8,2
		104	100	7,9
Gutenstein End	2011.09.18.	98	89	7,8
		92	87	7,5

Table 6: Calculated relative initial and end granted production data under Standard Test Condition of the panels and the efficiency of the panels.

3.3 Description of Sanyo data sources

In the planning period of the present study had been calculated with the production data of a Sanyo HIT heterojunction panel system. Finally, the data of the one half year in operation panel system could not be involved in this study. Thus, in this study it was calculated with production data provided by the producer and the financial background given by the implementation company.

4. Description of results

It must be made clear that the theme selected was to develop an in situ measurement method for testing amorphous photovoltaic panel degradation. To get general information from real life always involves difficulty. Although the in situ theme resulted in many unplanned circumstances and faults determined, the results were sufficient to point out advantages of the used test process and make some limited conclusions about tested panels. First of all in general the calculated productivity and efficiency results were in the expected band.

Secondly the changing tendencies were also well within the expectations supported by the literature discussed above.

4.1. Efficiency and production comparison of producers data and measured data

As seen on Table 5 both productivity and production indicators of our very limited measurements are around the data given by producer.

The column of "Ratio of granted and measured power P_{DC} " indicates by percentage the comparison of our measured production and what the producer indicated on their product description. P_{DC} shows the production before the losses of the converter.

Right after the panel's installation in Gutenstein the measured production was + 4-8 % higher than it is granted by the producer. Although it was not the target to see the converter efficiency, it is seen that electricity conversion from direct current to alternating current causes losses of - 4-8 %. The initial measurement on the other location shows less productivity. It should be taken into account that Vienna's 11st district initial measurement was the very first case and we learned many faults from it.

The total conversation efficiency from sun irradiation to direct current is 7,9 – 8,2 % in Gutenstein which correlates well to the calculated 8,04 % efficiency from the panels description.

The ratio of the producers granted productivity and the measured productivity after 45-90 days of intensive summer sun light expose shows poorer results. In the Vienna location the measured productivity is 4 % less than indicated by the panel description. In the Gutenstein location it has a relatively high 10-12 % productivity loss after 1 ½ months of sun expose. This poorer performance is also double checked by the alternating current measurement. Regarding our data in Gutenstein, the sun irradiation conversation to electricity efficiency dropped back in 45 days from 7,9-8,2 % to 7,5-7,8 %. The maximum system accuracy is 2,71%

4.2 Discussion of the results

One must consider that all results presented here are measured in situ. On one hand this has many advantages:

- Relatively large scale panel systems could be detected (36 panel each). Data from large scale systems has a kind of balance of the best and the worst panels, while in a

Master Thesis

MSc Program
Renewable Energy in Central & Eastern Europe

standard test normally only 1-2 panels are tested.

- At least a good average can be drawn from results from different locations (originally four locations). The original plan was to follow the first three summer months' panel performance of four different implementations. This could lead to many results, as degradation speed (curve) depends on irradiation intensity: points of the compass, angular offset, location average temperature. There are relatively large average temperature differences between Vienna's 3rd district and Gutenstein. The maximum hours of average sunshine in Vienna city center is 250 hours from July to August while in the Gutenstein area only in July reaches 200 hours average sunshine and it is much less in June (160 hours) and in August (180 hours). Details of weather differences in the Annexes.
- Exposure to the real life barriers. Not only the panel performance determines the level of electricity production, as discussed in Productivity and efficiency chapter.

On the other hand the disadvantages of the in situ measurements could strongly determine the results:

- Inability to repeat the measurement. This is very important in the initial measurement, when main part of the degradation occurs right after the exposition to the sun. This happened with the Vienna 3rd district location, when the inverter broke down and it was replaced many weeks afterwards. But also as the Vienna 11st district initial measurement was the very first attempt therefore many mistakes were committed which made the results from that location inaccurate. This is the reason why the initial Vienna 11st measurement is not in the expected order.
- Inability to record accurate data. In some cases it is difficult to read in the same moment the irradiation and the P_{DC} , P_{AC} or I_{mpp} , U_{mpp} plus panel temperature. In case of unsteady weather, especially when the irradiation changes rapidly it is impossible to get the right production data for the changing irradiation. In an in situ trial this has to be calculated with the timing constraints of the weather forecast, of the owner and also of the observer.
- In situ measurement cannot use a very accurate instrument. In case of these measurements the best accuracy for the system is 2,71 %.

Allowing for the above circumstances we can state the following.

In Gutenstein the average initial production of the 36 panels is over the producers granted production. The produced electricity is 104 -108 % of the accepted one. As a check the production of alternating current is 4 – 8 % less, which corresponds to the inverters'

Master Thesis

MSc Program
Renewable Energy in Central & Eastern Europe

maximum 95 % efficiency. The average initial measured panel efficiency also matches the data given by the producer.

After 1 ½ months production dropped back by 10 -12 %, which is better than expected from the literature of amorphous silicon panels, no producers' data was given; and as there are no data of micromorph degradation it is acceptable. In Vienna productivity after degradation was almost the same after three months (81 days) of summer sun exposition. Panel efficiency in Vienna also went back to 7,6 % from the granted 8,04% regarding to this measurement. It must be noted that the final measurement in Vienna was performed under circumstances of low irradiation.

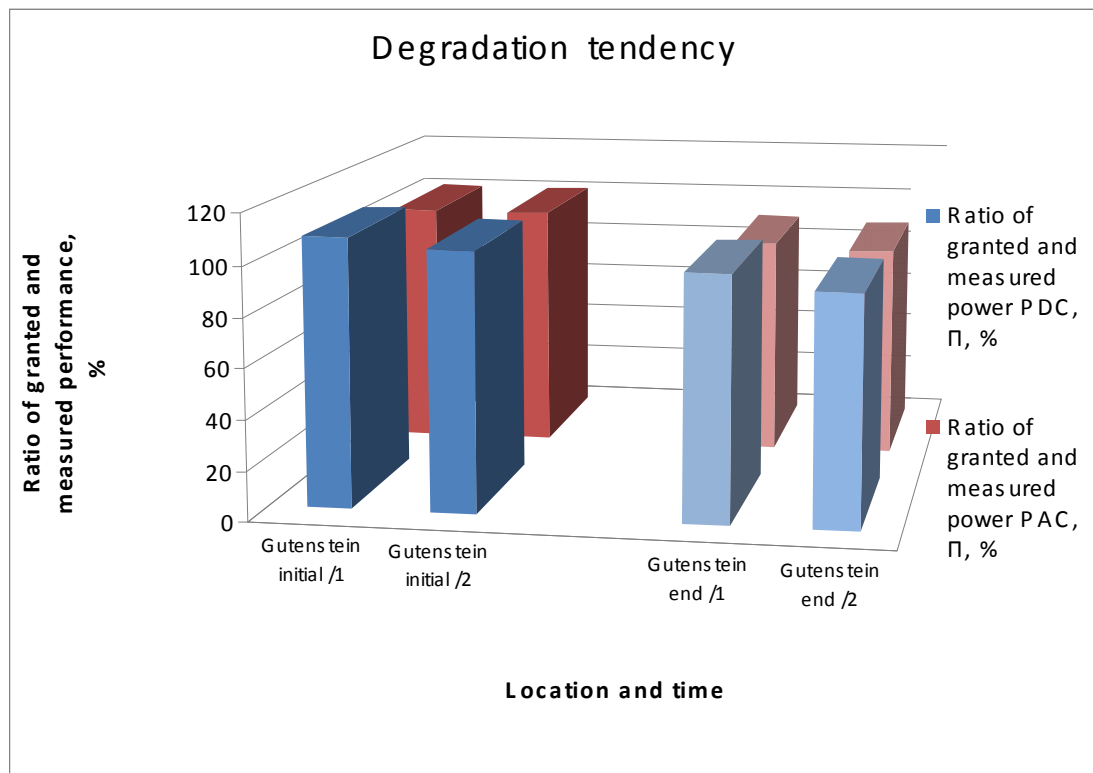


Figure 11: Relative productivity differences in Gutenstein after 1 ½ month of sun exposition.

All together, even given measurement difficulties, all the final data suggest that the relatively early and characteristic sunlight induced degradation of approximately – 10 %. The measurement system's best accuracy is 2,71%.

The NPV calculation shows that the NPV of the less efficient micromorph type panel turns to positive in the fourth year with 0,38 €/kW FIT (Feed in Tarif), while the more effective hetero-junction (Sanyo HIT Power 195) panels has positive NPV in the sixth year. After 20 years of operation the less effective series NPV is 31 870 € and the more effective Sanyo HIT Power 115 has +15 771 € (47 641 €) higher NPV.

5. Conclusion

We planned to develop a handy measurement process, applied in real life, for one of the most dynamically improving photovoltaic sectors, the thin film microcrystalline type cell. In cooperation with a PV systems installation company called Nikko-PV, which is located in Niederösterreich, south of Vienna, four locations were identified in a 60 km circle. Two of the locations (Vienna 3rd district and Pitten) are in “average” circumstances, one out of four has a warmer climate (+12% average temperature) with much more (+ 34%) August sunshine hours than the poorest shine covered location and colder climate (- 17% average daily August temperature). At all four locations we planned to install 30-36 panel (42-52 m²) of Bosch μ m-Si+ micromorph panels at private households during June. In this case there would be at least four times 2 ½ months panel performance data. Because of the difficulties of in situ trials, in the end we could only observe the first hundreds hours of sunlight induced degradation in two locations.

This type of in situ measurement had many advantages and also many disadvantages. The main disadvantage was that we had to study the entire process in situ and there was no opportunity to repeat the observations. The main advantage was that there were multiple locations and large sized panels (36 panels each) of PV performance involved in the measurement development process. The presented data and tendencies demonstrate real degradation, as it was double checked first by recording the power showed in the inverter in comparison with measured irradiation, and second by calculating the power before the inverter from the measured operating current and operating voltage.

During the measurement process many potential opportunities for mistakes could appear and influence or inhibit the result:

- failed implementation of some location
- failed initial measurement, no opportunity to repeat
- measurement at weak irradiation or in very changeable weather
- poor installation or calibration of measurement instruments
- no panel caused performance degradation

To get much more accurate data a more frequent or fluent production and irradiation recorder should be applied. Fluent monitoring would allow not only the detection of real performance for a longer period and the avoidance of measurement error, but also improved detection of seasonal changes.

Master Thesis

MSc Program
Renewable Energy in Central & Eastern Europe

Results reflect the expectation that micromorph panels also suffer serious light induced degradation. The degradation during our observations was around 10 %. In an earlier study (Chapter 1.3.3 Degradation) issued in 2003 the average LID was 12-14% of micromorph cells. This is approx. 10% degradation occurred after approx. 600 hours of sunshine exposure in the case of Vienna 11th district and after approx. 300 hours in the case of Gutenstein. In case of amorphous silicon degradation this amount of sunshine exposure was already sufficient to reach the majority of degradation (Fig. 5.). If we presume the same degradation curve of micromorph cells it is obvious that in practice large scale micromorph cells have less light induced degradation than amorphous. We also have to consider that many non LID circumstances may have also degraded the final results.

It would be very interesting to see if seasonal efficiency changes could also be detected at micromorph panels. Seasonal alternation should be detected in the upcoming winter and summer. Furthermore, it would be really interesting to find if amorphous based cells performed better in the warmer part of a Central European country.

6. References

[AIM] V. Avrutin, N. Izyumskaya, H. Morkoç: „Semiconductor solar cells: Recent progress in terrestrial applications”, *Superlattices and Microstructures*, Volume 49, Pages 337-364, 2011

[Bur] B. Burnett: “The Basic Physics and Design of III-IV Multijunction Solar Cells”, Denver, 2002

[Ener] <http://www.energy.eu/>

[Eurst] http://epp.eurostat.ec.europa.eu/statistics_explained/images/4/4f/Half-yearly_electricity_and_gas_prices_%28EUR%29.png

[FGC] R. Foster, M. Ghassemi, A. Cota: *Solar Energy*, CRC Press, Boca Raton, 2010

[Giga] <http://gigaom.com/cleantech/are-thin-film-solar-efficiency-standards-unfair/>

[KSW] M. Kaltschmitt, W. Streicher, A. Wiese: “Renewable Energy”, Springer, Berlin, 2007

[LH] A. Luque, S. Hegedűs: “Photovoltaic Science and Engineering”, Wiley, West Sussex, 2011

[Nrel] www.nrel.gov, http://www.nrel.gov/pv/performance_reliability/

[OMS] OMSZ, Országos Meteorológia Szolgálat

[Osbr] D. E. Osborn: “Overview of Amorphous Silicon Photovoltaic Installations at SMUD”, ASES Solar, Austin, 2003

[PA] J. Poortmans, V. Arkhipov: “The Film Solar Cells Fabrication, Characterization and Applications”, John Willey and Sons Ltd., West Sussex, 2006

[RD] C. Radue, E.E. van Dyk: “A comparison of degradation in three amorphous silicon PV module technologies”, *Solar Energy Materials and Solar Cells* 94, p. 617-622, 2010

Master Thesis

MSc Program
Renewable Energy in Central & Eastern Europe

[Raz] T. M. Razykov, et al: "Solar photovoltaic electricity: Current status and future prospects", *Solar Energy* 85, p. 1580-1608, 2011-09-14

[Reu] <http://www.reuters.com/article/2011/07/26/idUS291731277020110726>

[Ren] http://www.ren21.net/Portals/97/documents/GSR/REN21_GSR2011.pdf

[Shacell] A. V. Shah, editor: "Thin-film Silicon Solar Cells", EPFEL Press, Lausanne, 2010

[SD] A. V. Shah, C. Droz: „Thin-film Silicon: Photovoltaic and Large-area Electronics“, EPFEL Press, Lausanne, 2004

[Shatec] A. V. Shah et al: "Thin-film Silicon Solar Cell Technology", *Progress in Photovoltaics: Research and applications*, Special Issue, p. 113-142, 2004

[WCB] S. Wagner, D.e. Carlson, H.M. Branz. "Amorphous and Microcrystalline Silicon Solar Cells", National Renewable Energy Laboratory, Colorado, in the Electrochemical Society International Symposium, 1999.

[WikLc] Wikipedia: Low-cost photovoltaic cell, http://en.wikipedia.org/wiki/Low-cost_photovoltaic_cell

[WikSe] Wikipedia: Semiconductor, <http://en.wikipedia.org/wiki/Semiconductor>

[WikSW] Wikipedia: Staebler–Wronski effect, http://en.wikipedia.org/wiki/Staebler%E2%80%93Wronski_effect

[WikTf] Wikipedia: Thin Film Solar Cell, http://en.wikipedia.org/wiki/Thin_film_solar_cell

[WRK] C. R. Wronsky, B. Von Roedern, A. Kolodziej: „Thin Film Si:H-based solar cells“, *Vacuum* 82, p. 1145-1150, 2008

[Yan] B. Yan et al: "Hydrogenated Microcrystalline Silicon Single-Junction and Multi-Junction Solar Cells", in *Mat. Res. Soc. Symp. Proc. Vol. 762*, Material Research Society, 2003.

Master Thesis

MSc Program
Renewable Energy in Central & Eastern Europe

[ZAM] www.zamg.ac.at

<http://www.zamg.ac.at/fix/klima/oe71->

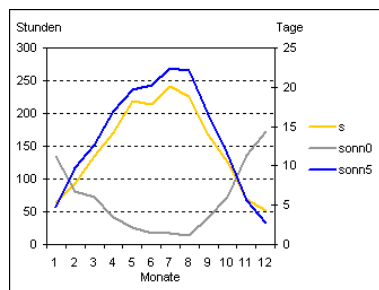
[00/klima2000/klimadaten_oesterreich_1971_frame1.htm](http://www.zamg.ac.at/fix/klima/oe71-00/klima2000/klimadaten_oesterreich_1971_frame1.htm)

[ZB] A. F. Zobaa, R. C. Bansal: "Handbook of Renewable Energy Technology", World Scientific, New Jersey, 2011

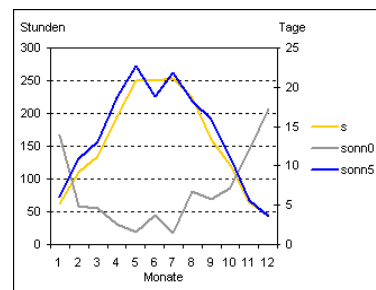
7. Annexes

7.1. Meteorology data of the locations

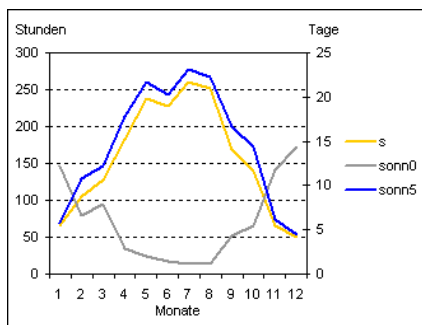
The following graphs and tables present some general information about the four locations where the panel performance and degradation was observed. The data are from the Austrian Meteorology Office (ZAMG) and represent the average of 30 years between 1971 and 2000. The observation stations and the location of PV panels with the bee-line distance to the observation stations are presented in brackets.



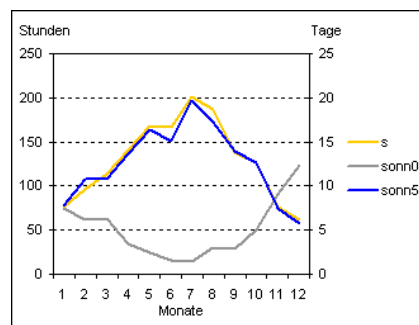
Wr. Neustadt (10 Km from Pitten)
altitude: 270 m



Gross-Enzersdorf (10 km from Vienna 11th dst)
altitude: 153 m



Vienna city center (10 km from Vienna 3rd dst)
altitude: 171m



Putzberg (10 km from Gutenstein)
altitude: 580 m

Abbreviations:

s = monthly average sunshine hours, h

sonn0 = number of days without sunshine, day

sonn5 = number of days with more than 5 hours sunshine, day

Figure 12: Sunshine differences of the locations [ZAM]

Master Thesis

MSc Program
Renewable Energy in Central & Eastern Europe

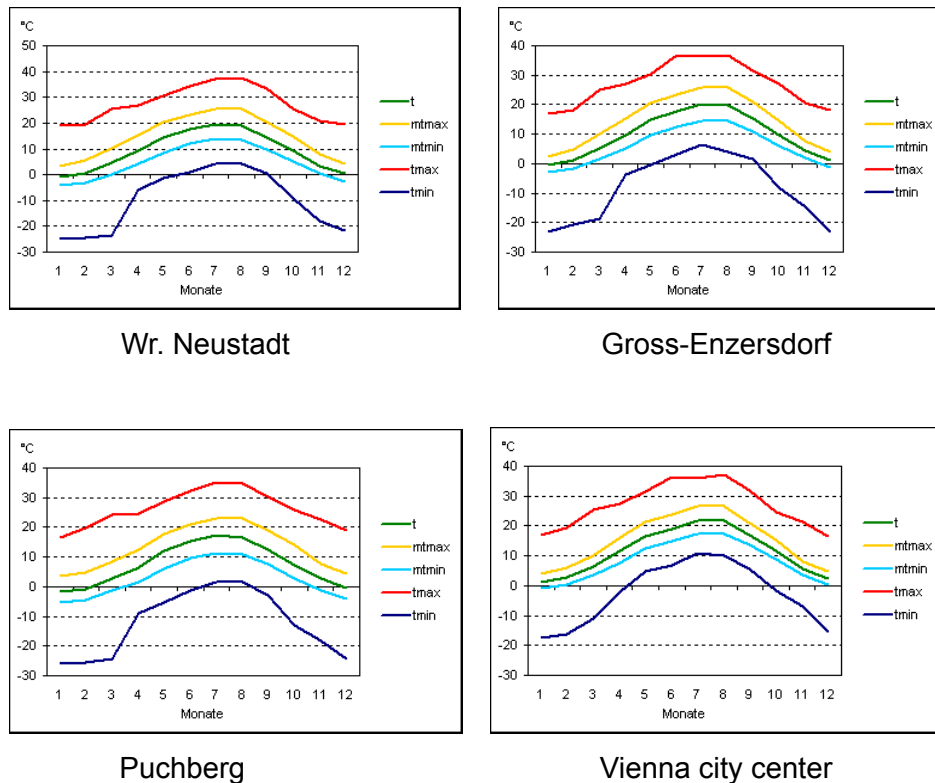


Figure 13: Average temperatures of the locations

7.2. Definition of some photovoltaic terminology

Air Mass

The air mass coefficient defines the direct optical path length through the Earth's atmosphere. The air mass coefficient can be used to help characterize the solar spectrum after solar radiation has traveled through the atmosphere.

AM 0: The spectrum outside the atmosphere, the 5,800 K black body, is referred to as "AM0", meaning "zero atmospheres".

AM 1: The spectrum after travelling through the atmosphere to sea level with the sun directly overhead is referred to, by definition, as "AM1".

AM 1,5: "AM1.5", 1.5 atmosphere thickness, corresponds to a solar zenith angle of $z=48.2^\circ$.

source: Wikipedia

Doping

Pure silicon has a certain size of band gap, which is 1,12 eV. In a given temperature in pure intrinsic silicon semiconductor the number of electrons and holes are equivalent. To decrease / increase or with other word adjust the band gap of semiconductor external materials are added to the silicon. With this method the number of electrons in the conduction band is

Master Thesis

MSc Program
Renewable Energy in Central & Eastern Europe

determined by the producer and the conductivity will be changed. The extra, impurity atom in the semiconductor can be either in the interstitial space of the host atoms or substitute some of the original atom. [FGC, p121]

The type of the impurity determinates the new conductivity of the new doped semiconductor. When a semiconductor e.g. silicon which has four valence electrons doped with an atom with three valence electrons (e.g. boron) the new alloy becomes an electron acceptor. Energy level of acceptors should be a little above of valence band. And in an inverse situation when the same silicon intrinsic semiconductor doped with an atom with four valence electrons the semiconductor becomes an **electron donor**. Energy level of donors should be a little bellow the conduction band.

The impurity atom could donate weaker bounded valence electrons, which means that these electrons can move relatively freely. Atoms (in group V) which have 5 valence electrons (e.g. phosphorus) act as electron donor as there is much less energy needed to release of a new electron. A semiconductor doped with such donor impurity is called **n-type** semiconductor. Bonding energy of boron in silicon is 0,045 eV, which means it creates “states” for electrons at the valence band. In other words, it creates a hole. The acceptor type doped semiconductors are called **p-type**. [WikSe]

Electron volt (eV) is the energy required to increase the electric potential (energy) of the charge on one electron by one volt.

Fill Factor (FF) the ratio of the actual maximum obtainable power, ($U_{mp} \times I_{mp}$) to the theoretical power, ($I_{sc} \times U_{oc}$). Typical commercial solar cells have a fill factor > 0.70 . Grade B cells have a fill factor usually between 0,4 to 0,7, high efficiency cells have a range 0,8 to 0,9. [KSW, p241]

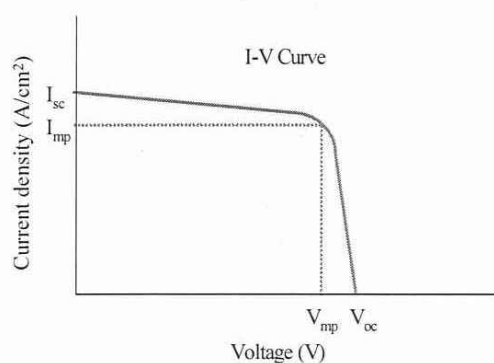


Figure 14: Fill factor: actual maximum obtainable power / theoretical power

Master Thesis

MSc Program
Renewable Energy in Central & Eastern Europe

Minority and majority carrier concentration is the term of the hole or electron concentration in a certain material.

Multi-junction solar cells, Categorization after the number of p-n junction

In a “single” p-n or p-i-n solar cell only the photons have been converted to electricity with the same or larger energy content than the band gap of the semiconductor. The energy of photons with less energy than band gap was lost, and the extra energy of the higher energy content photons was also lost. [LH, 12.5.1] Photons with less energy than the band gap usually transmitted through the material, while the excess energy of high energy content photons was usually dissipated as heat and wasted. The highest transfer efficiency was reached when the band gap and the photon’s energy were equal. [Bur, p11]

The basic concept behind multi-junction cells is **spectrum splitting**. In the first, top junction filters one part of the photons and the remaining photons that have smaller energy content than the band gap of the top layer pass it and are absorbed by lower layers. As the top layer has a relatively large band gap the first layer generates a relatively high open-circuit voltage through the whole cell from the top to the bottom junctions. It must be noted that in multi-junction cells no more photons can be absorbed than the bottom layer would absorb on its own. There is more incident power converted, however not more incident photons are absorbed. [LH, 12.5.1]

The simplest solar cell, called single solar cell, occurs when a p-n or even case of amorphous silicon p-i-n semiconductor is created.

As different types of semiconductors have different band gaps, different portions of the light can be converted to electricity.

In tandem cells e.g. nc-Si combined with a-Si, when a-Si with around 1,7 eV band gap converts the visible light energy content and leaves the infrared part lower energy content to nc-Si with a 1,1 band gap. The spectrum splitting advantages are more developed usage form following tandem cells is triple junction designs. [KSW, p250] For tandem and triple cells the p-i-n layers built on each other. The transportation of electrons in the tunnel junction is promoted by highly doped layers. In the p-n connection the n-doped layers functions as “bypas” the layers. This contact is called **tunnel contact**. The **voltage** on the p-i-n layers **added up**. [KSW, p250]

The second reason to build multi-junction cells is that in this way the uppermost layer could be thinner. This means that this layer has a better fill factor. [LH] Figure 3, which was created using empirical data, shows that as the thickness increases the FF decreases.

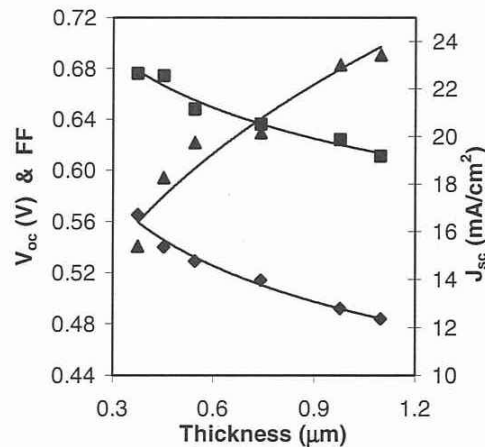


Figure 15: I-U (J-V) characteristics of $\mu\text{c-Si:H}$ single-junction solar cells versus the intrinsic layer thickness, where \blacksquare , \blacklozenge , and \blacktriangle denote FF, V_{oc} , and I_{sc} , respectively. It demonstrates that thinner thin film has a higher FF. [Yan, fig 1]

The volume of generated current also depends on the absorption coefficient of the material. The photogeneration layer thickness of all junction must be designed in such a way that the generated current is the same in all layers. The subcells should absorb the same number of electrons to produce the same amount of current. Thus, the output current is limited by the smallest output individual layer. The mobility of the electrons in amorphous silicon is lower than in crystalline. It has to be supported by an internal electric field. The thickness of each layer must be adjusted to be absorption constant so each layer produces the same current, therefore obtaining a **current matching**.

Multi-junction cells have lower operating current and higher operating voltage than single cells. The operation current is directly related to the number of photons used. Thus, with a lower band gap more photons can create more electron-hole pairs and thus more are available for current production. As multi-junction has more band gap layers, more current is generated than in a single junction, where only one band gap is higher. On the other hand as the number of layers increases the total current decreases as the photons need to cross increasing numbers of layers. In addition the electrons have to pass more layers, and these layers need to have greater electric potential.

The output voltage is directly related to the energy given by absorbed photons to the electrons moved from the valance band. Higher band gaps need more energy photons to get electrons to the conduction band.

With more cell layers the voltage of each layer summed with the others. This way the total voltage of multi junction cells is larger than that of single junction cells.

Master Thesis

MSc Program
Renewable Energy in Central & Eastern Europe

The electric resistive losses depend on the square of the current. This way the resistive loss can be significantly decreased when the current is lower. The total output of multi-junction can be higher than a single junction's because the voltage increase compensates more than the system's current decrease [Bur, p14].

Multi junction design must be considered in the structures of the different layers. **Lattice constant** is the distance between atoms in the crystal. **Mismatches** can happen in two cases: either where the lattice constant creates defects, or where dislocation recombination centers occur.

In the hetero-junction solar cells two or more different materials are in the same PV panel. The objective is similar to the multi-junction type panel: to increase efficiency by using different band gaps and also to eliminate or minimize light induced degradation. The commonly used hetero-junction method relies on crystalline wafer amorphous silicon layer [Shacell, p237]. *A i-type amorphous silicon layer between the crystalline base p- and n-type amorphous layers leads to less light induced degradation.*

By decreasing the layer thickness, we increase the relative electric field and improve electron mobility.

It seems that the thinner the i-layer, the lower the effect of light induced degradation will be [Shacell]. On the other hand the thickness of the two i-layers has to be combined. When both i-layers are too thin, a huge part of the energy will be lost, since not all will be absorbed [Shacell]. However, people must consider that very thin layers can absorb less light. Developing proper trapping surfaces in thin layers can be achieved with high stabilized efficiency. [WCB, p3] This was the third reason behind the strategy of the multi-junction cells. This phenomenon is one of the forces behind the construction of the multi-junction solar cell.

P-N junction

When the n-type semiconductor, which has an electron donor characteristic, and the p-type semiconductor, which has electron acceptor characteristic are matched together an interesting electrical behavior develops along this p-n junction. Between the p region and n region a concentration gradient exists because there are many more free electrons on the n-doped side of the junction than on the p-doped side.

This concentration gradient initiates diffusion: electrons movement from the high concentration region to the lower concentration region p-doped side. A significant number of the first free electrons are diffuse and recombine the holes: electrons create negative ions in the p-side. In the other n-side the converse process happens: holes are generated near the boundary and creates positive ions in the n-side. At the state when the concentration

Master Thesis

MSc Program
Renewable Energy in Central & Eastern Europe

gradient is equal to the electrostatic potential and the negative hole recombination stops. A stable region evolves near the junction boundary, where ions are present and mobile charges are not. This region is referred to as the depletion region.

Semiconductor is a type of material that has electrical conductivity performance between materials called conductor (e.g. Fe, Cu) and insulator (e.g. ceramics, rubber). The electrical conductivity could be described as the flow ability of electrons. The conductivity of semiconductors is between 10^3 and 10^{-8} siemens per centimeters. [WikSe]

The electrons inside the nucleus have discrete energy levels. There are a limited number of electrons that can occupy a certain energy level. In a crystal e.g. several electrons from different atoms can overlap each other and create an energy band. Also within these bands the number of places that can be occupied by electrons is limited: there is a finite energy state density. The innermost bands are the closest to the finite state. The electrons from this band cannot move freely, thus these electrons do not produce conductivity. These bands are referred to as **valence bands**. Electrons only move freely if they are in a band that is not in a finite state, not fully occupied. This band is referred to as a **conduction band**. Between these “allowed” energy bands there is an energy gap. [KSW, p229]

The electrons within different types of materials have different energy level. The electronic band structure of a material describes the status of the electrons. In insulator and semiconductor materials, the valence and conduction bands are separated by a relatively large band gap region. In insulator materials a great deal of energy is required to get electrons from the valence band to the conduction band. This amount of energy is described by the **band gap** energy (E_g). Band gap energy is the difference between the lowest energy level of the conduction band and the highest energy level of the valence band [Bur,6]:

- In insulators the band gap between conduction band and valence band is relatively large ($E_g > 3$ eV), the valence band is fully filled by electrons and the conduction band is empty. Only at very high temperatures a limited number of electrons able to overcome to conduction band.
- For semi conductors bands gap is smaller than in insulators ($0,1$ eV $> E_g > 3$ eV), and there are very few electrons on the conduction band in low temperatures. As the temperature increases, electrons are in a relatively excited status released from the valence band to the conduction band. Conductivity increases as the temperature rises (like winter 0 °C compared to summer 40 °C).
- With the metal conduction band and valence band overlapped, in metals there are electrons in conduction band. [WikSe, p36]. Freely moving electrons are within the

crystal lattice. Conductivity decreases as temperature increases, because the free electrons thermal oscillation increases. [RD, p618]

The semiconductors are further distinguished into “direct” and “indirect” semiconductors. For **direct semiconductors** only energy is required to get the electron from valence band to conduction band. For **indirect semiconductors** in addition to the energy of the photon an appropriate momentum is also needed for transfer to the conduction band. This is why in some types of semiconductors the photon needs to travel longer until it is absorbed. **Crystalline silicon is indirect semiconductor**, so it is needed to be relatively thick, while **amorphous silicon is direct semiconductor**. For crystalline silicon 200-300 μm thickness needed while for amorphous less than 10 μm thickness enough to transport same amount of electrons to conduction band. [KSW, p234]

Standard Sunlight Conditions are assumed as on a clear day 1 000 watts of solar energy per square meter ($1\ 000\ \text{W}/\text{m}^2$). This is also called as “one sun” or “peak sun”. Less sun creates less current. Standard Testing Condition (STC) is assumed i.e. $1\ \text{kW}/\text{m}^2$ irradiation, AM 1,5 spectrum and $25\ ^\circ\text{C}$.

Thickness, Classification by the semiconductors thickness

The silicon thickness can be several hundreds micrometer which are sliced from ingots. These are called wafer PVs.

Plasma-enhanced chemical vapor deposition (PECVD) is a process used to deposit thin films from a gas state (vapor) to a solid state on a substrate. The vapor contains silicon gas and hydrogen gas. As amorphous silicon itself is a semiconductor, a very thin layer (1 micrometer) is required in theory. In the practice silicon thin film has the diameter of some hundred of micrometers. Regarding to the deposition circumstances the film evolves from an amorphous phase to amorphous-microcrystalline and finally single microcrystalline phase. [PA, p193]

Microcrystalline silicon is another step to the direction from amorphous to crystalline silicon. Microcrystalline silicon consist crystalline silicon regions in an amorphous matrix. At a very high hydrogen dilution of the silicon forms the microcrystalline silicon at $200\text{-}250\ ^\circ\text{C}$. One big advantage of microcrystalline material is that the optical absorption of it is much higher than of monocrystalline because of internal scattering of the light. “Owing to efficient hydrogen passivation carrier recombination at grain boundaries is suppressed substantially and does not effect strongly the device performance.” [AIM, 4.2]

Master Thesis

MSc Program
Renewable Energy in Central & Eastern Europe

In the Figure 2 is presents schematically the structural transaction of hydrogen diluted silicon from protocrystalline through amorphous-microcrystalline to microcrystalline. The substrate temperature is constantly 200 °C. As the ratio of the silicon ($R = [H]/[SiH_4]$) in the hydrogen dilution rises the (a+ μ c)-Si:H layer and with higher silicon ratio μ c-Si:H layer continuously increases. The figure shows how thick protocrystalline-Si:H could be produced with a certain hydrogen/silicon dilution. It is also demonstrates that with increasing silicon ratio the nucleation (N_d) density is increasing and it is key to the subsequent growth of the (a+ μ c)-Si:H and later to the formation of μ c-Si:H.

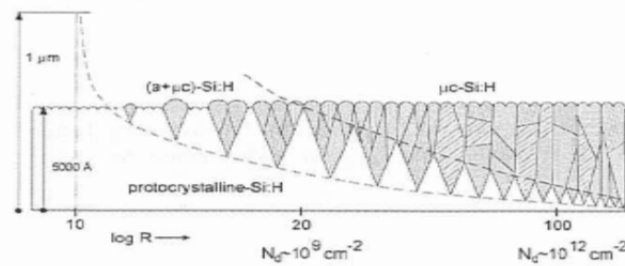


Figure 16: The amorphous-microcrystalline formation, transaction and thickness growth related to R ($R = [H]/[SiH_4]$) ratio and nucleation density (N_d). [WRK, p1146]